

Aus dem Institut der Toxikologie
der Universitätsmedizin der Johannes Gutenberg-Universität Mainz

Effects of chemotherapy with Temozolomide on cell cycle associated proteins in
Glioblastoma multiforme

Einfluss der Chemotherapie mit Temozolomid auf Zellzyklus und assoziierte Proteine
in Glioblastoma multiforme

Inauguraldissertation
zur Erlangung des Doktorgrades der
Medizin
der Universitätsmedizin
der Johannes Gutenberg-Universität Mainz

Vorgelegt von

Justus Rinke
Aus Eisenach

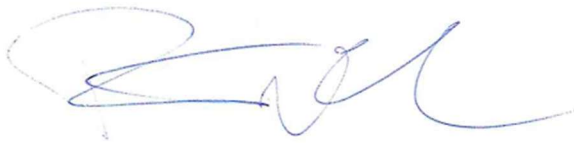
Mainz, 2023

Wissenschaftlicher Vorstand: Univ.-Prof. Dr. U. Förstermann
1. Gutachter: Univ.-Prof. Dr. rer. nat. Markus Christmann
2. Gutachter: Prof. Dr. Andrea Pautz
Tag der Promotion: 30. November 2023

Affidavit

I, Justus Rinke (students ID: 2726408) hereby confirm that this doctoral thesis entitled "Effects of chemotherapy with Temozolomide on cell cycle associated proteins in Glioblastoma multiforme" is my own work, which I have prepared independently and only with the help of the listed aids. Any parts of the thesis whose intellectual property has been taken in meaning or wording from other printed sources or from the internet have been clearly indicated by me. Furthermore, I confirm that this work has not yet been submitted in another examination procedure in the same or similar form and that plagiarism will in any case lead to the expiry of this declaration.

Mainz, March 2023



Justus Rinke

Contents

List of abbreviations	I
List of Figures	II
List of Tables	III
1. Summary	
2. Introduction	
2.1. Glioblastoma Multiforme and current best treatment	
2.2. Senescence, the Senescence-associated secretory phenotype, and its role in glioblastoma	
2.3. The cellular mechanism of TMZ treatment	
2.4. The DREAM-complex and its partners	
3. Literature review	
3.1. Senescence- friend or foe?	
3.2. O-6-methylguanin-DNA-methyltransferase deficient glioblastoma and their response to Temozolomide	
3.3. The DREAM complex and its components, B-Myb and fork head box protein M1	
4. Materials and Methods	
4.1. Cell lines	
4.2. Chemicals used	
4.3. Solutions	
4.4. Reaction kits	
4.5. Antibodies	
4.6. Primers	
4.7. Consumables and supplies	
4.8. Devices	
4.9. Software	
4.10. Cultivation of cells	
4.11. Seeding of cells	
4.12. Drugs and drug treatment	
4.13. Quantification of cellular senescence by flow cytometry	
4.14. β -Galactosidase staining	
4.15. Colony formation assay	
4.16. Extraction of proteins	
4.17. Bradford assay	
4.18. SDS gel electrophoresis and Western transfer	
4.19. Immunoblotting	
4.20. Gene transcription analysis; mRNA isolation	
4.21. Gene transcription analysis; Quantitative polymerase chain reaction	
5. Results	
5.1. Influence of TMZ on LN229 cells	
5.1.1. Cell-cycle distribution, senescence induction and clonogenic survival after treatment of LN229 cells with TMZ	
5.1.2. Gene expression analysis after treatment on LN229 cells with TMZ	
5.1.3. Protein expression analysis after treatment of LN229 cells with TMZ	

5.1.4. β -Catenin expression after Treatment of LN229 cells with TMZ and MG132 proteasome inhibition

5.1.5. β -Galactosidase assay after treatment of LN229 cells with TMZ

6. Discussion

6.1. Chemotherapy with Temozolomide

6.2. TMZ induces senescence and polyploidy in LN229 cells

6.3. Important changes in the transcriptome

6.4. Conclusion

7. Sources and literature

8. Appendices

9. Thanks

10. Resume

List of abbreviations

APS	Ammonium persulfate
BSA	Bovine serum albumin powder
CNS	Central nervous system
DDR	DNA Damage Response
DMEM	Dulbecco's Modified Eagle's Medium/Nutrient
DMSO	Dymethyl sulfoxide
DSB	Double Strand Break
E2F1	E2F transcription factor 1
E2F2	E2F transcription factor 2
E2F3a	E2F transcription factor 3a
E2F4	E2F transcription factor 4
E2F5	E2F transcription factor 5
ECL	Pierce™ ECL Western Blotting Substrate
EDTA	Ethylenediaminetetraacetic acid
EtOH	Ethanol
FCS	Fetal calf serum
FOXM1	Forkhead box protein M1
GSC	Glioblastoma stem cell
HCl	Hydrochloric acid
IDH1	Isocitrat-dehydrogenase 1
IDH2	Isocitrat-dehydrogenase 2
IL6	Interleukin 6
IL8	Interleukin 8
K3[Fe(CN)6]	Potassium hexacyanoferrate (III)
K4[Fe(CN)6]	Potassium hexacyanoferrate (II)
MeOH	Methanol
MgCl ₂	Magnesium chloride
MGMT	O ⁶ -methylguanin-DNA-methyltransferase
MMP-2	Matrix-metalloproteinase 2
Na ₂ HPO ₄	Dinatrium-hydrogen-phosphat
Na ₃ VO ₄	Sodium orthovanadate
NaCl	Sodium chlorite
NP-40	Nonidet™ P 40 Substitute
O ⁶ -MeG	O ⁶ -methylguanin
PBS	Phosphate buffered saline
PI	Propidium iodide
RBBP4	RB Binding Protein 4
RT	Room temperature
SASP	Senescence associated secretory phenotype
SDS	Sodium dodecyl sulfate
β-gal	5-bromo-4-chloro-3-indolyl-β-Dgalactopyranoside
STAT3	Signal transducer and activator of transcription 3
TEMED	Tetramethylethylenediamine
TMZ	Temozolomid

Tris
Trypsin/EDTA
List of figures

Tris(hydroxymethyl)aminomethane
Trypsin-Ethylenediaminetetraacetic acid

- Figure 1 Progression of the inhibiting DREAM complex and the activating B-MYB/MuvB, FOXM1/MMB, FOXM1/MuvB complexes during cell cycle.
- Figure 2 Dose response of LN229 cells after treatment with TMZ. SubG1 and Cell cycle distribution after treatment with TMZ.
- Figure 3 β -Galactosidase assay of LN229 cells after treatment with TMZ.
- Figure 4 Colony forming assay: Colony formation of LN229 cells after treatment with TMZ.
- Figure 5 Quantitative qPCR evaluation of CCL2, CCL8, CXCL1, IL6, IL8, CCNA2, CENPF, p21, E2F1, Exo1, FANC1, FOXM1 HMGB1, HMGB2, LMNB1, MYBL2 after TMZ treatment.
- Figure 6 Quantitative qPCR evaluation of CCND2, FANCC, FANCF, IL1A, IL1B and CCNA1 after TMZ treatment.
- Figure 7 Western transfer analysis of LN229 cells after treatment with TMZ.
- Figure 8 Western transfer analysis for β -catenin on earlier timepoints.
- Figure 9 Western transfer analysis for β -catenin with MG132 inhibition.

List of tables

Table 1	chemicals
Table 2	solutions
Table 3	reaction kits
Table 4	antibodies
Table 5	primers
Table 6	consumables and supplies
Table 7	devices
Table 8	software
Table 9	seperation gel
Table 10	stacking gel
Table 11	temperature profile qPCR

1. Summary

[German/Deutsch]

Diese Arbeit befasst sich mit Mechanismen der zellulären Seneszenz in LN229 Glioblastoma Zellen infolge der Behandlung mit Temozolomid (TMZ). Zum jetzigen Zeitpunkt ist das Glioblastoma multiforme noch immer eine infauste Prognose, bei der das Überleben eher in Monaten als in Jahren geschätzt wird. Seneszente Zellen verlieren zwar ihre Teilungsfähigkeit und tragen damit nicht direkt zur Ausweitung einer malignen Tumormasse bei, sie beeinflussen jedoch weiterhin ihre Umgebung durch die Sekretion unterschiedlicher Faktoren, wie Entzündungsmediatoren. Dieser Einfluss ist oft nachteilhaft für den Patienten und kann sich somit negativ auf die Therapie auswirken. Daher sollen im Rahmen dieses Projektes, die Mechanismus der zellulären Seneszenz nach TMZ-Behandlung untersucht werden. Im Detail befassen wir hierbei mit der Rolle des DREAM-Komplexes, ein Haupt-Regulator des Zellzyklus, sowie der Rolle assoziierter Proteine welche eine Rolle im Zellzyklus und der Seneszenz spielen.

In Rahmen der vorliegenden Arbeit, konnte die TMZ-induzierte Seneszenz in LN229 Zellen nachgewiesen werden. Weiterhin zeigten wir eine deutliche Erhöhung in der FOXM1 Expression, sowohl auf RNA wie auch auf Proteinebene, sowie eine Erhöhung von MYBL2 und EXO1 auf RNA-Ebene. Die Bedeutung dieser Regulierung im Zusammenhang mit der Seneszenz wird diskutiert.

[English]

This thesis deals with mechanisms of cellular senescence in LN229 glioblastoma cells as a result of treatment with temozolomide (TMZ). At the time of writing this, glioblastoma multiforme are still a grim diagnosis with the remaining survival even with best current treatment often measured in months rather than years. While senescent cells cease division and therefore do not contribute to an expansion of tumour cells directly, they influence their surroundings in a variety of ways, like the secretion of different factors, such as inflammatory mediators. Therefore, senescence can be directly harmful to the patient and not conducive to treatment. Therefore, within the framework of this project, the mechanism of cellular senescence after TMZ treatment will be investigated. We focus on components of the DREAM complex, a protein complex that acts as a master regulator of cell cycle progression, as well as on associated proteins connected to cell cycle progression or the senescent state.

In the present work, TMZ-induced senescence was detected in LN229 cells. Furthermore, we showed a significant increase in FOXM1 expression, both at RNA and protein level, as well as an increase in MYBL2 and EXO1 at RNA level. The significance of this regulation in the context of senescence is discussed.

2. Introduction

2.1. Glioblastoma Multiforme and current best treatment

Glioblastoma multiforme are the most common malignant tumours arising from the brain itself, more specifically the astrocytes. While they typically form in the brain's cerebral hemispheres, they can be found anywhere in the brain and even in the spinal cord. The tumour cells tend to grow quickly and often find access to the dense system of blood vessels that supply the central nervous system. If left untreated, glioblastoma multiforme lead to death within an average of six months after diagnosis. Even with swift diagnosis and best current treatment, the diagnosis is still grim and the average patient's survival of 15 months [1]. Common symptoms arise mostly from the tumour growing to take space in the skull, both with its bulk of cells as well as by inducing capillary leak in the blood vessels of its vicinity, leading to oedema and necrosis often found at its centre. These symptoms often include, but are not limited to nausea, headaches, blurred vision, seizures, lack of appetite, instability in both mood and personality, difficulty speaking [2]. Glioblastoma make up about 14.5 % of central nervous tumours of the central nervous system (CNS) as well as 49 % of all malignant tumours of the CNS [1].

Gliomas, the larger category involving glioblastoma, are histologically separated into four grades- grade I and grade II, known as astrocytoma, are slow-growing and in comparison, less aggressive. The other side of the scale, grades III and IV are malignant and characterised by a high proliferation rate (grade III) and the presence of necrotic tissue, often with angiogenic activity (grade IV). The WHO classification of 2021 further contains characteristics established by molecular analysis, such as isocitrat-dehydrogenase 1 (IDH1)/ isocitrat-dehydrogenase 2 (IDH2) mutant, IDH1/IDH2 wildtype and O⁶-methylguanin-DNA-methyltransferase (MGMT) promotor methylation, among others. Of those, IDH1/IDH2 wildtype is typical for primary grade IV glioblastoma, while IDH1/IDH2 mutation is primarily found in secondary glioblastoma. MGMT methylation shows an inverse relation, being found more often (although not exclusively) in secondary glioblastoma [3]. The cancer cells of glioblastoma however are characterised by a high level of genetic instability and the tumour itself can contain cell populations carrying vastly divergent mutations, further selected for by their specific microenvironment [4,5]. LN229 cells, used in our experiments here and in other projects of our group, are MGMT methylated and IDH wildtype [6].

First line therapy for glioblastoma consists of resection whenever possible and subsequent radiotherapy (IR) of the peritumoral region [7,8]. In conjunction with the radiotherapy, if there are no contraindications, Temozolomide (TMZ) is used as cytostatic drug [7,8]. However, for patients receiving the full extent of this multimodal treatment strategy, the median survival remains rather short at only 14.6 months (specifically for WHO grade IV astrocytoma, histologically confirmed) [9]. Glioblastoma multiforme are known for a heterogenous cell population in biopsy as well as a micro infiltrative pattern of growth. Together with general hyper-vascularity this makes complete excision almost an impossibility - especially considering the tight confines to vital brain matter most often found in its vicinity.

Recurrence is the typical problem when facing therapy of glioblastoma [9] and such recurrent

tumours often harbour mutations that have been shown to be linked to the treatment with alkylating agents [10]. Beyond the selection caused by the treatment itself, the short timeframe of recurrence after therapy calls for further research into glioblastoma and their response under standard therapy. In this work, we will specifically focus on chemotherapy with TMZ.

TMZ is a triazene derivative that decomposes spontaneously after application, not needing metabolic activation. The decomposition yields 3-methyl-(triazene-1-yl)imidazole-4-carboxamide, then 5-aminoimidazole-4-carboxamide and monomethyl hydrazine. Monomethyl hydrazine is an alkylating chemical species that induces the formation of a variety of methylation products in the DNA- more specific to exposed *Oxygen* and *Nitrogen* atoms of the bases. These alkylated DNA bases differ not just in position of the adduct, but also in their stability and toxicity. O⁶-methylguanine (O⁶-MeG), formed by alkylation of the normal guanine at the O⁶ position, shows the most cytotoxic potency - if not repaired, it will lead to double-strand breaks (DSB) [11,12]. This is despite the fact O⁶ methylations make up only a small fraction of all alkyl DNA bases [13]. Exposure of tumour cells to clinically relevant doses of TMZ cause sufficient accumulation of DNA damage ultimately result in either cell death or senescence [14], with senescence specifically being of interest, since the cells remain in place and continue to influence the situs.

2.2. Senescence, the Senescence-associated secretory phenotype, and its role in glioblastoma

Senescent cells are characterised by a stable cell cycle arrest; they do not return to proliferation even if stimulated by appropriate mitogenic stimuli.

There are a many pathways to senescence, by both internal and external stimuli. The first description of senescent cells by Hayflick and Moorhead in 1961, described replicative senescence- essentially a stable cell cycle arrest after subculturing cells roughly 50 times [15]. Replicative senescence is caused by shortening telomers [16]. Besides repeated cell duplication without telomere restoration, senescence can also be induced prematurely by oncogenic stimuli [17] and cellular stress [18]. During embryological development, physiological senescence is important for differentiation [19].

Metabolic changes of cells going into senescence include differentiation in protein synthesis, increased glycolysis and generation of reactive oxygen species as well as deregulated fatty acid oxidation [20,21,22]. The DNA undergoes extensive heterochromatinization [23] and the cells show extensive transformation in morphology, with a generally larger and more plump looking cell structure.

Senescence is a tumour suppressive mechanism [24], as it disrupts a potentially malignant cell in its replicative potential. Relevant to this, many premalignant transformations contain senescent cells as well [25].

Senescent cells express the Senescence-associated secretory phenotype (SASP) [26], reshaping their own microenvironment by autocrine and paracrine signalling, as well as enzymatically. This toolbox plays a role in a variety of physiological processes, most prominent of which being tissue repair [27]. In case of glioblastoma, the resulting microenvironment might play a decisive role in progression or the recurrence after treatment.

Additionally, research has shown that a stable bypass of senescence is possible in a variety of different cell lines [28,29,30]. This could imply senescent cells as a source of recurrence. But even if in vitro the senescence-like state is a common endpoint, senescent cells might be present at the earliest point of treatment- when samples from untreated mouse glioblastoma

xenografts were checked for markers of senescence, a significant fraction of otherwise untreated xenograft glioblastoma cells showed senescence associated biomarkers as well [31], so glioblastoma are likely under the influence of the SASP even before treatment has commenced. The influence of senescent cells and the SASP is currently subject to a lot of discussion and research. A conclusion has yet to be reached, however a purely positive influence on tumour suppression by senescence seems unlikely [32].

SASP components can be tumour suppressive but can also contribute to progression [33,34]. The pro-tumorigenic properties are in part due to the changes in the cancer's vicinity, e.g. due to secretion of matrix-degrading proteases, increasing cell motility and stimulating cell growth and division [34]. The accumulation of senescent cells, independent of what mechanism induced their senescence, might therefore contribute to carcinoma progression.

A reason for tumour progression can be found in the inflammatory secretome produced by the senescent cells as part of the SASP. Interleukin 6 (IL6) and interleukin 8 (IL8) are commonly associated with senescent cells and their contribution to the SASP [34,35]. They are pivotal proinflammatory cytokines and contribute to the microenvironment via recruitment of different immune cells, depending on the cytokine and with certain overlap. For the case of glioblastoma, there are further characteristics of IL6 and IL8 of interest.

IL6 in fact seems necessary for the development of high-grade glioblastoma in transgenic mice, as shown by Weisenberger et al., 2004 [36]. Here, IL6 activated the Signal transducer and activator of transcription 3 (STAT3) pathway, after binding to the IL6 receptor and the common signal transducing receptor glycoprotein 130 (gp130); both receptors are found on glioblastoma cells and confer a growth- and survival advantage to the tumour [37]. STAT3 activation promoted invasion and migration in several glioblastoma cell lines (U251, T98G and U87MG) [38]. STAT3 was also associated with an increased expression of matrix-metalloproteinase 2 (MMP-2), that increases invasion in U87MG glioblastoma [39]. Interestingly, MMP-2 induction can also be caused by FOXM1 [40]. IL 8 has also been found to increase angiogenesis and invasion in some glioblastoma cell lines [41, 42]. Most functions of IL8 follow CXCR1 or CXCR2 binding, but so far glioblastoma cells have only been found expressing CXCR1 [42]. In glioblastoma, non-senescent cells can start secreting IL6 and IL8 as well, induced by hypoxia [43,44]. Since glioblastoma are solid tumours with a high rate of proliferation, hypoxia is fairly common and associated with poorer overall survival [45], likely due to a variety of factors.

Ouchi et al., 2016 [32] found, that senescent GBM146 and GBM 157 glioblastoma cells secrete Vascular Endothelial Growth Factor (VEGF) -A and -C, supporting angiogenesis (as well as potentially Glioblastoma stem cell (GSC) differentiation to endothelial cells, capable of forming functional vasculatures). VEGF released by senescent cells fairly likely plays a role in the angiogenesis in and around glioblastoma (as well as potentially GSC differentiation to endothelial cells, capable of forming functional vasculatures [32]). These cells were not kept under hypoxic conditions.

2.3. The cellular mechanism of TMZ treatment

During DNA replication, the methylation of guanine at the O⁶-position will change the hydrogen bonding, causing mispairing or non-Watson-Crick pairing as O⁶-MeG pairs with thymine (O⁶MeG / T) [46]. These mismatches are subject to the mismatch repair-pathway

(MMR), consequently thymine is excised but reinsertion of thymine causes replication stressing lesions and ultimately replication-mediated DNA double-strand breaks [47]. The enzyme responsible for repair of O⁶-MeG is MGMT [48, 49]. Studies show, that MGMT promotor methylation (and therefore a reduction in DNA repair capacity) has a significant positive influence on post treatment survival for glioblastoma patients [50]. DSBs are known to cause senescence in proliferating cells, as well as cell death [51, 52].

Senescence caused by O⁶-MeG, has been shown to arrest the cell cycle at the G2/M check point and to be dependent on the Ataxia telangiectasia and Rad3 related MRN- ATR pathway. The permanent cell cycle arrest depends on p53 protein induced p21 protein accumulation [14].

2.4. The DREAM-complex and its partners

The DREAM complex has long been identified as a regulator in cell cycle progression. In its most complete form, found primarily during cellular quiescence, the MuvB complex with LIN9, LIN37, LIN52 and LIN54 as well as RB binding protein 4 (RBBP4) associates with the retinoblastoma-like pocket proteins p107 and p130 in their hypophosphorylated form as well as E2F transcription factor 4 (E2F4) with its dimerization partner DP1, all together forming in the DREAM complex. During quiescence, the DREAM complex binds to almost all genes relevant for cell cycle progression, including those relevant for early cell cycle progression [53]. As long as p21 inhibits the cyclin/cyclin-dependent kinase complex by binding to it, p130/p107 remains hypophosphorylated and does not dissociate from its position. In this assembly, the DREAM complex suppresses E2F dependent promotion of G1-/S-phase gene transcription [53]. After the dissociation of p130, the MuvB core binds to B-MYB, forming a complex that promotes genes relevant for the S-phase [54,55]. Afterwards, the B-MYB/MuvB complex recruits forkhead box protein M1 (FOXO1) after the phosphorylation of B-MYB by cyclin dependent kinase 2. This enables expression of FOXO1 target genes during G2 [54]. Target genes of FOXO1 associated with the B-MYB/MuvB complex then enable the G2-M transition [54]. Genes for the early cell cycle progression are mostly targets of E2F Transcription Factor 1, E2F transcription factor 2 and E2F transcription factor 3a [56].

B-Myb binds and inhibits the p16 promotor and is suppressed during senescence [57]. Lastly, to induce cell cycle arrest, p53 mediates a switch of the MuvB core associated components from B-MYB protein complex back to the DREAM complex [58].

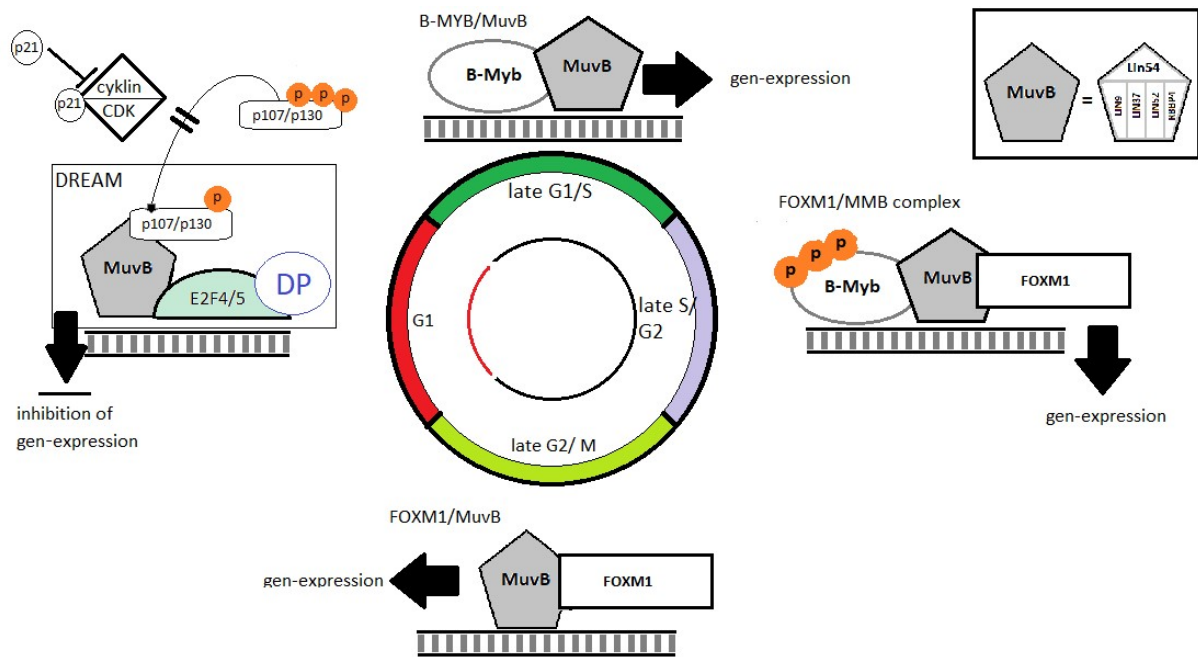


Figure 1: **Progression of the inhibiting DREAM complex and the activating B-MYB/MuvB, FOXM1/MMB, FOXM1/MuvB complexes during cell cycle.** The DREAM complex during quiescence suppresses the expression of G1-/S-phase associated genes. Hyperphosphorylation of p130 causes the DREAM-complex to disband; the MuvB core associates with B-MYB, forming B-MYB/MuvB, activating the expression of genes relevant to late G1 and S phase. Transitioning into G2, FOXM1 joins the complex forming the FOXM1/MMB complex, that activates the expression of genes relevant to the late S and G2 phase. After entry into the G2 phase, B-Myb dissociates and the FOXM1/MuvB complex remains, activating the expression of genes relevant to the late G2 and M phase. Adapted from Mowla, Sophia & Lam, Eric & Jat, Parmjit. (2014). Cellular senescence and aging: The role of B-MYB. *Aging Cell*. 13. 10.1111/ace1.12242.

2.5. Goal of this project:

Previous work of the Christmann group showed that, in glioblastoma cells, TMZ is only mildly cytotoxic, but strongly cytostatic. Thus, TMZ induces senescence at a high frequency. A similar phenotype was observed in breast cancer cells upon treatment with the environmental carcinogen B[a]P. In this case senescence was mainly caused by p21-mediated inactivation of CDK4 and subsequent activation of the DREAM complex.

The goal of the present PhD thesis was to analyse the role of the DREAM complex in TMZ-induced senescence in the glioblastoma cell line LN229. Therefore, in a first step the TMZ-induced irreversible cell cycle arrest in the G2/M phase and senescence induction will be verified using FACS-analysis, β -Gal staining, and the colony formation assay. In a next step, TMZ-induced alteration in senescence-, DREAM- and cell proliferation-associated factors will be analysed on RNA and protein level using qPCR and Immunodetection, respectively. From the alteration of these factors, conclusions concerning the impact of the DREAM complex on TMZ-induced senescence will be drawn.

3. Literature Review

3.1. Senescence- friend or foe

Senescence, and specifically the senescence of cancer cells has been of interest to research in recent years. The exact molecular definition of the senescent cell and what defines it is still somewhat debated [60], but several indicators have found broad acceptance and use [21,23,59,60]. The same goes for the question rather or not senescence is beneficial or not; in some cases, it can be answered rather convincingly, such as in the case of embryonal senescence [19] or wound regeneration [27]. For early carcinogenesis, research suggest senescence plays the role of a tumour suppressor [24,25,26]. But in the case of later stages of carcinoma, a conducive answer is highly unlikely [26,31,32,33,34]. Overall, there is less research arguing for, than against an overall positive effect on survival. In the case of glioblastoma, the general trend of the research presented suggests a negative impact [31].

3.2. O⁶-methylguanin-DNA-methyltransferase deficient glioblastoma and their response to Temozolomide

Glioblastoma multiforme show a wide variety of clinically relevant mutations; LN229 cells in particular lack expression of O⁶-methylguanin-DNA-methyltransferase (MGMT) due to promoter methylation. This epigenetic silencing is of importance for predicting the response to therapy and is therefore well covered in current research [3, 47, 50, 61]. LN229 cells also lack expression of p16 due to a deletion mutation, a protein of relevance in regard to some research concerning senescence [62, 63]. All senescence induction characterised in research so far is dependent on p53 and p21 [62, 63, 64].

Senescence in glioblastoma multiforme is broadly researched, both regarding the molecular signalling chains and to its influence on patient survival. In the case of LN229 cells specifically, our group is actively conducting research, establishing senescence as the primary response of LN229 cells to therapy with TMZ [65].

3.3. The DREAM complex and its components, B-Myb and fork head box protein M1

The different components of the DREAM are well known as a master regulator of cell cycle [53,58]. Investigation of B-Myb and fork head box protein M1 (FOXM1) showed them to be able to delay the onset of senescence [57,66,67,68,69,70] and in some cases they were involved in the reversal of a senescence like state [28]. FOXM1 specifically has been shown to increase the tumorigenicity in glioblastoma [71].

4. Materials and methods

4.1. Cell lines

For this project, we used LN229 cells. LN229 cells were purchased from American Type Culture Collection (ATCC) and were described in terms of TMZ responses in a previous publication [72]. The LN229 cell line expresses mutant, but functional p53, but neither express MGMT, nor p14 or p16 [6]. Cultivation was carried out in Dulbecco's Modified Eagle's Medium/Nutrient (DMEM) containing 10 % FCS at 37°C in humid atmosphere supplemented with 5 % CO₂ and checked routinely for mycoplasma contamination using the Venor®GeM Classic Mycoplasma Detection Kit.

4.2. Chemicals used

[Table 1: chemicals used]

Chemical	Abbreviation where applicable	Manufacturer
5-bromo-4-chloro-3-indolyl- β -Dgalactopyranoside	β -gal	Sigma Aldrich, München
Acrylamide (37.5:1)		Carl Roth GmbH + Co. KG, Karlsruhe
Ammonium persulfate	APS	Carl Roth GmbH + Co. KG, Karlsruhe
β -mercaptoethanol		Carl Roth GmbH + Co. KG, Karlsruhe
Bovine serum albumin powder		BSA Carl Roth GmbH + Co. KG, Karlsruhe
Bradford reagent		Carl Roth GmbH + Co. KG, Karlsruhe
Citric acid		Carl Roth GmbH + Co. KG, Karlsruhe
Crystal violet		Carl Roth GmbH + Co. KG, Karlsruhe
Dymethyl sulfoxide	DMSO	Carl Roth GmbH + Co. KG, Karlsruhe
Disodium-hydrogen-phosphate	Na ₂ HPO ₄	Carl Roth GmbH + Co. KG, Karlsruhe
Dry-milk powder		AppliChem GmbH, Darmstadt
Dulbecco's Modified Eagle's Medium/Nutrient	DMEM	Sigma Aldrich, München
Ethanol	EtOH	Carl Roth GmbH + Co. KG, Karlsruhe
Ethylenediaminetetraacetic acid	EDTA	Carl Roth GmbH + Co. KG, Karlsruhe

Fetal calf serum	FCS	PAN-Biotech GmbH, Aidenbach
Formaldehyde solution (37 %)		Carl Roth GmbH + Co. KG, Karlsruhe
Giemsa stain		Sigma Aldrich, München
Glutaraldehyde solution (50 % wt)		Sigma Aldrich, München
Glycine		Carl Roth GmbH + Co. KG, Karlsruhe
Hydrochloric acid	HCl	Carl Roth GmbH + Co. KG, Karlsruhe
Isopropanol		Carl Roth GmbH + Co. KG, Karlsruhe
Magnesium chloride	MgCl ₂	Carl Roth GmbH + Co. KG, Karlsruhe
Methanol	MeOH	Carl Roth GmbH + Co. KG, Karlsruhe
Nonidet™ P 40 Substitute	NP-40	Honeywell Fluka™ by Thermo Fisher Scientific, Braunschweig
PageRuler™ Prestained Protein Ladder, 10 to 180 kDa		Thermo Fisher Scientific, Braunschweig
Phosphatase Inhibitor Cocktail 2 (P5726)		Sigma Aldrich, München
Phosphate buffered saline	PBS	Biochrom GmbH, Berlin
Pierce™ ECL Western Blotting Substrate	ECL	Thermo Fisher Scientific, Braunschweig
Potassium hexacyanoferrate (II)	K ₄ [Fe(CN) ₆]	Sigma Aldrich, Munich
Potassium hexacyanoferrate (III)	K ₃ [Fe(CN) ₆]	Sigma Aldrich, Munich
Propidium iodide (1 mg/ml)	PI	Sigma Aldrich, München
RNase (10 mg/ml)		Sigma Aldrich, München
Roti®-Load 1 (4x)		Carl Roth GmbH + Co. KG, Karlsruhe
Sodium chloride	NaCl	Carl Roth GmbH + Co. KG, Karlsruhe
Sodium dodecyl sulfate	SDS	Carl Roth GmbH + Co. KG, Karlsruhe
Sodium orthovanadate	Na ₃ VO ₄	Sigma Aldrich, München

Spectra™ Multicolor Broad Range Protein Ladder C		Thermo Fisher Scientific, Braunschweig
Temozolomid	TMZ	Prof. Geoff Margison, Centre for Occupational and Environmental Health, University of Manchester, Manchester
Tetramethylethylenediamine	TEMED	Carl Roth GmbH + Co. KG, Karlsruhe
Tris(hydroxymethyl)aminomethane	Tris	Carl Roth GmbH + Co. KG, Karlsruhe
Trypsin-Ethylenediaminetetraacetic acid	Trypsin/EDTA	Sigma Aldrich, München
Tween® 20 T		Carl Roth GmbH + Co. KG, Karlsruhe
Western Lightning® Plus-ECL		PerkinElmer, Inc., Waltham (USA)

4.3. Solutions

[Table 2: solutions]

Solution/buffer	Components
BSA solution (5 %)	1.25 g BSA powder 25 ml TBST
Citric acid/Na ₂ HPO ₄ buffer (40 mM) pH 6.0	36.85 ml Citric acid (0.1 M) 63.15 ml Na ₂ HPO ₄ (0.2 M)
Colony staining solution (1x)	1000 ml dH ₂ O 1.25 g Crystal violet 12.5 ml Giemsa stain
Culture medium (LN229) 500 ml DMEM	500 ml DMEM 50 ml FCS
Fixation solution (10x, β-Galactosidase assay)	8.1 ml Formaldehyde solution (37 %) 0.6 ml Glutaraldehyde solution (50 %) 6.0 ml PBS (25x) 0.3 ml dH ₂ O

Laemmli buffer (5×)	30 g Tris 144 g Glycine ad 1 l dH ₂ O
Milk solution (5 %)	5 g Dry-milk powder 100 ml TBST
Lysis buffer	25 µl Tris-HCl (1 M, pH 8.0) 10 µl EDTA (500 mM) 10 µl PMSF 2 µl DTT 1 µl Na ₃ VO ₄ 50 µl NP40 143µl Protease inhibitor 10 µl Phosphatase inhibitor 100µl NaCl 659µl dH ₂ O
Propidium iodide (50 µg/ml)	2.5 ml PI stock solution (1 mg/ml) 47.5 ml PBS
RNase (0.1 mg/ml)	300 µl RNase stock solution (10 mg/ml) 30 ml PBS
Running buffer (SDS electrophoresis buffer, 1×)	200 ml Laemmli buffer (5×) 5 ml SDS (20 %) 795 ml dH ₂ O
SDS (20 %)	20 g SDS ad 100 ml dH ₂ O
Staining solution (1×, β-Galactosidase assay)	10 ml Na ₂ HPO ₄ /citric acid (pH 6) (40 mM) 1 ml NaCl (1.5 M) 1 ml MgCl ₂ (20 mM) 100 µl [K ₃ Fe(CN) ₆] (500 mM)

	100 µl [K ₄ Fe(CN) ₆] (500 mM) 200 µl X-gal (2 %)
Transfer buffer (blotting buffer, 1×)	100 ml Laemmli buffer (5×) 200 ml MeOH ad 1 l dH ₂ O
Tris-buffered saline (TBS, 10×) pH 7.6	24.2 g Tris 80 g NaCl ad 1 l dH ₂ O
Tris-buffered saline with Tween [®] 20 (TBST)	100 ml TBS (10x) 2 ml Tween [®] 20 ad 1 l dH ₂ O

4.4. Reaction kits

[Table 3: reaction kits]

Reaction kit	Manufacturer
GoTaq [®] qPCR Master Mix	Promega, Madison (USA)
NucleoSpin [®] RNA	Macherey-Nagel, Düren
Verso cDNA Synthesis Kit	Thermo Fisher Scientific, Braunschweig

4.5. Antibodies

[Table 4: antibodies]

Antibody	kDA	Organism	Serial number	Dilution	Manufacturer
Anti-mouse IgG, horseradish peroxidase coupled	-	Goat	610-1302	1:2000	Rockland Immunochemicals, Philadelphia (USA)
Anti-rabbit IgG, horseradish	-	Goat	611-1302	1:2000	Rockland Immunochemicals, Philadelphia (USA)

peroxidase coupled					
β-Actin	43	Mouse	sc-47778	1:2000	Santa Cruz Biotechnology, Dallas (USA)
B-Myb	79	Rabbit	SAB4501939	1:1000	Sigma Aldrich, München
β-Catenin	92	Rabbit	ab32572	1:1000	Abcam, Cambridge (UK)
CyclinD1	34-37	Rabbit	ab134175	1:1000	Abcam, Cambridge (UK)
E2F1	47	Rabbit	ab5391	1:1000	Abcam, Cambridge (UK)
E2F4	53	Mouse	sc-511	1:1000	Santa Cruz Biotechnology, Dallas (USA)
E2F5	38	Mouse	sc-374268	1:1000	Santa Cruz Biotechnology, Dallas (USA)
FOXM1	104 – 122	Mouse	sc-271746	1:1000	Santa Cruz Biotechnology, Dallas (USA)
H3K9me2	15	Rabbit	ab32356	1:1000	Abcam, Cambridge (UK)
H3K9me3 Chip grade)	17	Mouse	ab1220	1:1000	Abcam, Cambridge (UK)
HMGB1	29	Rabbit	6893	1:500	Cell Signaling Technology, Massachusetts (USA)
HMGB2	24	Rabbit	ab 67282	1:1000	Abcam, Cambridge (UK)
HSP90	90	Mouse	sc-13119	1:2000	Santa Cruz Biotechnology, Dallas (USA)
LIN9	62/64/58	Mouse	sc-398234	1:1000	Santa Cruz Biotechnology, Dallas (USA)

LMNB1	67	Mouse	sc-365962	1:1000	Santa Cruz Biotechnology, Dallas (USA)
p130	130	Rabbit	ab 68136	1:1000	Abcam, Cambridge (UK)
p21	21	mouse	554228	1:1000	BD Bioscience, (UK)
pp130	130	Rabbit	ab 68136	1:1000	Abcam, Cambridge (UK)
pRB	106	Rabbi	t 8516	1:1000	Cell Signaling Technology, Massachusetts (USA)
RB	106	Rabbit	sc-050	1:1000	Santa Cruz Biotechnology, Dallas (USA)
TP53INP1	25 – 37	Rabbi t	ab 202026	1:1000	Abcam, Cambridge (UK)

4.6. Primers

[Table 5: primers]

<i>Target gene</i>	Sequences of primer (5`-3`)	
<i>CCL2</i>	Forward	CCTTCATTCCCAAGGGCTC
	Reverse	CTTCTTTGGGACACTTGCTGC
<i>CCL8</i>	Forward	TGTCCAAGGAAGCTGTGAT
	Reverse	TGGAATCCCTGACCCATCTCT
<i>CCNA1</i>	Forward	GGACAGTGCTAGGGCTGCTA
	Reverse	GGAAGGCATTTTCTGATCCA
<i>CCNA2</i>	Forward	GTCTAGCGCAGCAGCAGAG
	Reverse	TGAACGCAGGCTGTTTACTG
<i>CCND2</i>	Forward	GGACATCCAACCCTACATGC
	Reverse	CCAAGAAACGGTCCAGGTAA
<i>CENPF</i>	Forward	GGCTAGCTGGAGAGTTGCAG

	Reverse	TTTGTGCATGCAATCTAGGC
<i>CXCL1</i>	Forward	CTGGCTTAGAACAAAGGGGCT
	Reverse	TAAAGGTAGCCCTTGTTCCTCC
<i>E2F1</i>	Forward	ATGGTGATCAAAGCCCCTCC
	Reverse	AAACATCGATCGGGCCTTGT
<i>EXO1</i>	Forward	ATTGGACATTATCTCAAGATG
	Reverse	GCTGATAGAGGAAGGTATT
<i>FANCC</i>	Forward	AGATGTATGAAGCCTTGAA
	Reverse	AGACAACATAAGCACCAT
<i>FANCF</i>	Forward	GACAGACCTCTTATTAGC
	Reverse	CATTGCCTATACAGAACT
<i>FANCI</i>	Forward	GCTGTCTGGTTCTCATCT
	Reverse	CCGTATAGTTCAGGCTCTTA
<i>FOXM1</i>	Forward	GCAGCATCAAGCAAGAGATG
	Reverse	GCCGCTCAGACACAGAGTTC
<i>HMGB1</i>	Forward	GTTCAAGGATCCCAATGCAC
	Reverse	GCAACATCACCAATGGACAG
<i>HMGB2</i>	Forward	GCGGAATTCTCCAAGAAGTG
	Reverse	CTCCCTGTCATAGCGAGCTT
<i>IL1A</i>	Forward	TCTTCTGGGAAACTCACGGC
	Reverse	GCACACCCAGTAGTCTTGCT
<i>IL1B</i>	Forward	TGAGCTCGCCAGTGAAATGA
	Reverse	AGATTCGTAGCTGGATGCCG
<i>IL6</i>	Forward	GCTGCAGGACATGACAACCTC

	Reverse	AACAACAATCTGAGGTGCC
<i>IL8</i>	Forward	CCAAACCTTTCCACCCAAA
	Reverse	CTCTGCACCCAGTTTTCTT
<i>LMNB1</i>	Forward	AAGTGCAAGGCGGAACAC
	Reverse	TCGAATTCAGTGCTGCTCA
<i>MYBL2</i>	Forward	TGCTGTGGGTTCTAGCCTCT
	Reverse	AGATGGTTCCTCAGGGAGGT
<i>p21</i>	Forward	ACTCTCAGGGTCGAAAA
	Reverse	CGGCGTTTGGGAAGTGTA

4.7. Consumables and supplies

[Table 6: consumables and supplies]

Consumables and supplies	Manufacturer
Aluminium foil	Carl Roth GmbH + Co. KG Karlsruhe
Barriofilm® premium barrier foil	Carl Roth GmbH + Co. KG Karlsruhe
Cell culture dishes (6 cm, 10 cm)	Sarstedt AG & Co. KG, Nümbrecht
Cell culture flasks Cellstar® (25 cm ³)	Greiner Bio-One GmbH, Kremsmünster (Austria)
Cryo.s™ (cryotubes)	Greiner Bio-One GmbH, Kremsmünster (Austria)
Eppendorf Reference (manual single-channel pipette, 1 – 10 µl)	Eppendorf AG, Hamburg
Flow cytometry tubes	Sarstedt AG & CO KG, Nümbrecht
Glass Pasteur pipettes	Carl Roth GmbH + Co. KG, Karlsruhe
Hard-Shell® PCR Plates 384-well, thin wall, clear shell/white well (384-well plates)	Bio-Rad, Hercules (USA)

Hard-Shell® PCR Plates 96-well, thin-wall, white shell/clear well (384-well plates)	Bio-Rad, Hercules (USA)
Laboratory bottles	Schott AG, Mainz
Magnetic stirring bar	Carl Roth GmbH + Co. KG, Karlsruhe
Microseal® 'B' PCR plate sealing film	Bio-Rad, Hercules (USA)
Mini PROTEAN® Tetra Cell (gel electrophoresis chamber)	Bio-Rad, Hercules (USA)
Mini Trans-Blot® Cell (blotting chamber)	Bio-Rad, Hercules (USA)
Mini-PROTEAN® short plates	Bio-Rad, Hercules (USA)
Mini-PROTEAN® spacer plates (1.5 mm)	Bio-Rad, Hercules (USA)
Neubauer improved	Marienfeld-Superior, Lauda-Königshofen
Nitrile gloves (counting chamber)	Semperit AG Holding, Wien (Austria)
Nitrocellulose membrane	GE-Healthcare, Little Chalfont (UK)
Nunclon™ Delta Surface 6-well plates	Thermo Fisher Scientific, Braunschweig
Parafilm	Bemis Company, Inc. (USA)
Pipetboy 2 (pipet aid)	INTEGRA Biosciences AG, Biebertal
Pipet-Lite XLS+ (manual single-channel pipette)	Mettler Toledo, Columbus (USA)
PIPETMAN® (manual single-channel pipette, various sizes)	Gilson International B.V. Deutschland, Limburg an der Lahn
Pipette tips (10 µl – 1000 µl)	Greiner Bio-One GmbH, Kremsmünster (Austria)
Rainin AUTOREP E (repetitive pipette)	Mettler-Toledo GmbH, Gießen
Rainin Classic (manual single-channel pipette, various sizes)	Mettler-Toledo GmbH, Gießen
Reaction tubes (0.1 ml, 1.5 ml, 2.0 ml)	Eppendorf, Hamburg
Reaction tubes (15 ml, 50 ml)	Greiner Bio-One GmbH,

	Kremsmünster (Austria)
RNase AWAY™ (RNase and DNA decontamination agent)	Molecular BioProducts Inc by Thermo Fisher Scientific, San Diego (USA)
ROTILABO® blotting paper (Whatman paper), 1.0 mm thick	Carl Roth GmbH + Co. KG, Karlsruhe
Serological glass pipettes (5 ml, 10 ml)	Carl Roth GmbH + Co. KG, Karlsruhe
Serological plastic pipettes CellStar® (5 ml, 10 ml)	Greiner Bio-One GmbH, Kremsmünster (Austria)
SurPhob SafeSeal® filter tips	Biozym Scientific GmbH, Hessisch Oldendorf
Venor® Gem Clasic Mycoplasma Detectikon kit for conventional PCR	Minerva Biolabs

4.8. Devices

[Table 7: **devices**]

Device	Name	Manufacturer
Centrifuge	Galaxy Mini (for 1.5 ml reaction tubes)	Merck Eurolab, Darmstadt
	Heraeus Megafuge 1.0	Thermo Fisher Scientific, Braunschweig
	Heraeus Megafuge 1.0R	Thermo Fisher Scientific, Braunschweig
	Heraeus Megafuge 16R (with cooling function)	Thermo Fisher Scientific, Braunschweig
Clean bench	MSC-Advantage™	Thermo Fisher Scientific, Braunschweig
CO ₂ incubator	Heracell™ 150	Thermo Fisher Scientific, Braunschweig

Flow cytometer	BD FACS Canto II	BD Biosciences, San Jose (USA)
Magnetic stirrer	MR2002	Heidolph Instruments GmbH & Co.KG, Schwabach
Microplate reader photometer	Sunrise™	Tecan Trading AG, Männedorf (Switzerland)
Microscope	ECHO Rebel (camera function)	Discover Echo Inc., San Diego (USA)
	Axiovert 40 C	Carl Zeiss, Jena
pH meter	pH211 Microprocessor	Hanna Instruments Deutschland GmbH, Vöhringen
Platform shaker	Rocker 25	Labnet international inc, Edison, NJ (USA)
Power supply	PowerPac™ Basic	Bio-Rad, Hercules (USA)
	PowerPac™ HC	Bio-Rad, Hercules (USA)
	PowerPac™ Universal	Bio-Rad, Hercules (USA)
Precision scale	TE4101	Sartorius, Göttingen
qPCR system	CFX384™ Real-Time System	Bio-Rad, Hercules (USA)
Roller shaker	Roller Mixer SRT9	Stuart, Stone (UK)
Thermal cycler	T100™ Thermal Cycler	Bio-Rad, Hercules (USA)
Thermal mixer	Thermomixer compact	Eppendorf AG, Hamburg
UV-Vis spectrometer	NanoDrop 2000	Thermo Fisher Scientific, Braunschweig
Vortexer	ZX4 Advanced IR Vortex Mixer	VELP Scientifica Srl, Usmate Venate (Italy)
Water bath	Grant Instruments™ JB1	Grant Instruments, Cambridge (UK)

Western blot detection system	iBright CL1000	Invitrogen™ by Thermo Fisher Scientific, Carlsbad (USA)
-------------------------------	----------------	---

4.9. Software

[Table 8: software]

Software	Developer
Accelrys Draw V4.1	Symyx Technologies, Santa Clara (USA)
BD FACSDiva™	BD Biosciences, San Jose (USA)
CFX Manager™	Bio-Rad, Hercules (USA)
CorelDRAW X7 V17.1.0.572	Corel Corporation, Ottawa (Canada)
GIMP 2.10.32	GIMP Development Team
GraphPad Prism 6	Graphpad Sioftware, La Jolla (USA)
ImageJ V1.53i	Wayne Rasband (NIH), Maryland (USA)
Magellan™ V7.2	Tecan Trading AG, Männedorf (Switzerland)
MS Office 365	Microsoft, Washington D.C. (USA)
NanoDrop Operating Software	Thermo Fisher Scientific, Braunschweig
Photoshop® 7.0	Adobe Inc., Mountain View (USA)

4.10. Cultivation of cells

For cultivation, cells were seeded on 10 cm² cell culture dishes or in 25 cm² cell culture flasks. For experimentation, cells were transferred to 10 cm² cell culture dishes or 6-well plates and incubated at 37 °C in an atmosphere of 5% CO₂. To avoid full confluence, the cell culture had to be split at least twice a week. For splitting cell-cultures, the culture medium was removed. Afterwards the adherent cells were washed with 5 ml PBS to remove remaining culture medium. To remove the cells from their surface, 1 ml of Trypsin/EDTA in the case of a 10 cm² dish and 25 cm² cell culture flasks, or 0.5 ml for a 6 cm² dish, was added to the cells. Following 4 min of incubation at 37 °C at 5% CO₂, the cells were detached from the surface of the dish and floating, confirmed visually using a microscope. Once cells were detached, the enzyme was inactivated using cell-culture medium, ad 10 ml. Cells were separated by pipetting up and down. Finally, the cells were seeded for continued cell cultivation or experiments in a ratio according to cell-count as determined using the microscope.

4.11. Seeding of cells

Cells were seeded in defined cell numbers. To determine the amount, we used a Neubauer counting chamber. 10 μl of the cell suspension was pipetted on the chamber that was divided into squares of equal area. After counting the cells in the four different squares, the mean value was calculated. To determine the actual concentration of cells per ml, the average cell count per square was multiplied by $10^4 \frac{1}{\text{ml}}$.

The cells were then seeded in different concentrations depending on the size of the dish, planned treatment and time until harvest.

4.12. Drugs and drug treatment

TMZ was dissolved in DMSO (22,2 mg/ml stock) and stored in batches at -80°C until use. Before use, 900 μl of the stock was diluted with 2013 μl sterilized, distilled water and added to the cell culture medium according to the desired concentration. Water-diluted stocks were used once only.

4.13. Quantification of cellular senescence by flow cytometry

Flow cytometry measures both size and granularity of individual cells as they quickly flow through a laser beam, allowing for these values to be determined for large populations. Size is measured in the form of forward scatter value, while granularity shows as the side scatter value. The measurements of each cell can be plotted, therefore allowing the measurement of distinct populations and their subpopulations. Different fluorescent probes can be used, for example Propidium Iodide, as it intercalates DNA and can be measured separately. This in turn allows statements over cell cycle distribution [73].

To determine the cell cycle distribution of LN229 cells upon TMZ exposure, cells were exposed 24 h after seeding to TMZ in concentrations of 10 μM , 25 μM , 50 μM and 100 μM . Cells were harvested after 144 h. All cells were harvested, including attached and floating cells. Because dead LN229 cells tend to float in the culture medium, the entirety of said medium, was collected in a 15 ml reaction tube first. Next the well was washed with 3.5 ml PBS, collecting the liquid in the same reaction tube as the old medium. To detach the LN229 cells from their well, 1 ml Trypsin/EDTA was added to the 10 cm wells and after incubation at 37°C in 5 % CO_2 , the added enzyme was deactivated with 1 ml of culture medium (DMEM). Next, the suspended cells were transferred into the same tube as the corresponding culture medium and the whole mixture was centrifuged for 5 min at $1500 \times g$. For further work on the cell pellets, the liquid phase was carefully removed, and the remaining pellet washed with 2 ml of PBS. Most of the 2 ml of PBS were removed, and a to remnant of liquid was left allow the cell pellet to be resuspended in a liquid phase (gentle pipetting). Then, it was fixed by slow addition of 3 ml ice-cold, 70 % ethanol.

To allow flow cytometry, the cells were again centrifuged for 5 min at $1500 \times g$ and the supernatant removed. After evaporation of the ethanol, RNase in PBS (ad 330 μl) was added. The cells were resuspended and transferred to a flow cytometry tube and left to incubate for 30 min.

In the last step of preparation, 170 μl of the DNA intercalating agent PI (50 $\mu\text{g}/\text{ml}$ in PBS) were added into the tubes. For transport to the BD FACS Canto II, all cytometry tubes were stored on ice in a closed lid plastic bucket. A minimum of 10000 cells were counted on the machine. BD FACSDiva™ was used for data analysis and GraphPad Prism 6 for visualisation.

4.14. β -Galactosidase staining

Positive staining for senescence associated β -Galactosidase activity at an unphysiological pH was used as another indicator of senescence. To determine the senescence of cells under TMZ treatment, β -Galactosidase staining was used. SA(Senescence-associated)- β -Galactosidase cleaves X-gal into β -galactose and 5-bromo-4-chloro-3-hydroxyindole. Under aerobic conditions, this molecule will dimerise and form the blue dye 5,5`dibromo-4,4`-dichloro-indigo [74]. Cells were seeded on 6-well plates for ease of handling. After 24 hours, the cells were exposed to TMZ at concentrations of 10 μM , 25 μM , 50 μM and 100 μM respectably, then incubated for another 120 hours as describe above under cultivation of cells. Next, the culture medium was removed, and the cells were washed twice with roughly 2 ml PBS. For fixation of the cells, 1 ml of the fixation solution [Table 2] was added and remained 5 min at room temperature (RT). Subsequently, to remove remnant fixative solution, the cells were washed once briefly and then twice for 5 min each with 2 ml PBS per well. To stain the cells, 1 ml of freshly prepared staining solution [Table 2] was added to each individual well. Since it is not soluble, it remains visible on affected cells under the microscope. The 6-well plates were then stored at 37°C under CO₂ exclusion. As to avoid staining of non-senescent cells, the incubation was stopped after 17 hours, the staining solution removed, and the wells washed twice with 2ml PBS. All wells were covered in 2 ml PBS and stored at 4 °C. For the evaluation of the β -Galactosidase assay, images were taken using the ECHO Rebel microscope camera at 20 times magnification. A minimum of 500 cells per well were photographed and counted using ImageJ, determined to be senescent or not by blue stain. Finally, the percentage of senescent cells was determined.

4.15. Colony formation assay

The colony formation assay allows for an assessment on the survivability and viability of treated cells. LN229 cells were seeded at low densities (100 cells on 6 cm² dish). 6 hours after seeding, the cells were treated with TMZ. Afterwards, they were incubated at 37 °C and 5 % CO₂ for 2 weeks.

After the colonies had grown, the culture medium was removed. The dishes were washed with roughly 2 ml of PBS before the cells were fixed with 2 ml of methanol. Following 5 min of incubation, the methanol was removed. Next, the LN229 cells were stained using 2 ml of crystal violet for 10 min. Once the dye was removed and the dishes were washed once again, newly formed colonies, indicating viable cells at the time of seeding, were visible and could be counted manually.

4.16. Extraction of proteins

Whole cell extracts were used for Western blot analysis. Cell cultures for whole cell extracts were seeded onto 10 cm cell culture dishes and treated with 50 μM TMZ 24 hours after seeding. To generate whole-cell extracts form 10 cm cell-culture dishes at 96 hours and

144 hours, first the culture medium was siphoned off. After this, the cells were washed twice with 5 ml PBS to remove remaining culture medium. To remove the cells from the surface of their cell culture dish, 1 ml of trypsin/EDTA was added into the dish. Following 4 min of incubation at 37 °C at 5 % CO₂, roughly 8-9 ml TRIS-HCL was added as to better transfer the now non-adherent cells from their dish. The natant cells were then transferred into a 15 ml Eppendorf tube using a 10 ml pipette. To generate cell pellets from the resulting solution, the 15 ml tubes were centrifuged at 10.000 x g for 10 min. After siphoning off the supernatant, the remaining precipitated fraction, from here on referred to as the cell pellet, was frozen and stored at -80 °C.

To prepare the extracts for further analysis, each cell pellet was suspended in 1 ml of lysis buffer. They were placed into an overhead shaker and incubated for 15 min. at 4 °C. The supernatant was transferred into a 1.5 ml Eppendorf tube and stored at -18 °C for later experimentation.

4.17. Bradford assay

Before cell-lysates can be used for Western blot analysis, they had to be equilibrated. For this, the total protein concentration of the lysates was determined using the Bradford protein assay [75]. First, depending on estimated protein concentration, the lysates were diluted between 1:2 and 1:10 using dH₂O. For this assay, 1.5 µl protein lysate per well were distributed onto a 96-well plate. Each protein extract checked was included in duplicate. Different BSA concentrations (0, 1, 2, 3, 4, 5 µg/ml) in duplicate were used for the standard curve. 200 µl of Bradford reagent was added to each well used in the assay.

Following 10 min of incubation at room temperature, the absorbance was measured at 620 nm and the protein concentration was determined by linear regression via Excel.

4.18. SDS gel electrophoresis and Western transfer

Before the samples were loaded into the gel pockets, 30 µg of protein were first filled up to 30 µl with dH₂O and subsequently 10 µl of 4x loading buffer were added. Following denaturation for 5 min at 95 °C, the samples were loaded into the gel pockets of the collection gel. The collection gel was situated on top of a separating gel of 7.5 %, 10 % or 12 % SDS concentration [Table 9 /Table 10]. An appropriate separating Gel was chosen regarding the estimated size of the protein in question. For verification of separation during electrophoresis (Mini PROTEAN® Tetra Cell) and as a reference size of the proteins, 5 µl of Spectra™ Multicolour Broad Range Protein Ladder was loaded into one of the gel pockets. The gels ran for 2 h at 70 mA. The proteins were transferred to a 0.2 mm cellulose membrane in a Mini Trans-Blot® Cell blotting chamber using plotting buffer. First, two sponges and three Whatman filter papers were soaked in transfer buffer [Table 2]. From anode to cathode starting with a sponge, followed by two layers of filter paper on which the nitrocellulose membrane was placed. On top the membrane, the gel was placed and smoothed to remove any remaining air bubbles. Another layer of filter paper and sponge for a total of three layers of filter paper were added. The blotting cassette was closed and placed in the chamber (Mini Trans Blot® Cell). After filling up with transfer buffer and adding an ice pack, blotting was carried out for 1.5 h at 300 mA.

[Table 9: **separating gel**] *amount sufficient for a maximum of three gels*

Chemical	7.5 % separating gel	10 % separating gel	12 % separating gel	15 % separating gel
dH ₂ O	13.0 ml	11.4 ml	13.0 ml	8.6 ml
1.5 M Tris (pH 8.8)	6.0 ml	6.0 ml	6.0 ml	6.0 ml
Acrylamid 37:1	4.6 ml	6.0 ml	4.6 ml	9.0 ml
20 % SDS	120 µl	120 µl	120 µl	120 µl
APS	120 µl	120 µl	120 µl	120 µl
TEMED	12 µl	120 µl	12 µl	12 µl

[Table 10: **stacking gel**] amount sufficient for a maximum of four gels

Chemical	Collection gel
dH ₂ O	8.8 ml
0.5 M Tris (pH 6.8)	1.5 ml
Acrylamid 37:1	1.5 ml
20 % SDS	120 µl
APS	120 µl
TEMED	12 µl

4.19. Immunoblotting

To avoid unspecific binding of antibodies, the loaded membranes were then blocked using 5 % non-fat dry milk, 0,1 % polysorbate (TWEEN) or, for detecting phosphorylated proteins, 5 % Albumin for 1h. Next, the membrane was incubated with the appropriate antibody as listed [Table 4] in 5 % non-fat dry milk or, in the case of phosphorylated proteins, 5 % Albumin overnight at 4 °C. Afterwards the membranes were washed and incubated with anti-mouse or anti-rabbit IgG coupled horseradish peroxidase for 1 hour at room temperature. The Antibody/protein complexes were visualized with ECL Amersham Pharmacia Biotech, following their protocol.

4.20. Gene transcription analysis; RNA isolation

The RNA was extracted from 30 mg of cell samples. First, cells underwent RNA purification with the NucleoSpin® RNA kit, following their protocol. The cells, isolated via centrifugation, were lysated by direct addition of 350 µl of Buffer RA1 from the kit and 3.5 µL β-mercaptoethanol. After that, the mixture was vortexed. For filtration, the lysate was put into a NucleoSpin® Filer provided in the kit over a collection tube. After centrifugation at 11,000 x

g for 1 min, the filter was removed, and the filtrate homogenized using 350 μ l of ethanol 70% by pipetting up and down 10 times. To bind the RNA, the homogenized filtrate was put into NucleoSpin[®] RNA Column placed into a Collection Tube. After centrifuging at 11,000 x g for 30 s, the column was placed into a fresh Collection Tube. To make the rDNase digest more effective, the silica membrane inside the NucleoSpin[®] column was desalinated using 350 μ l Membrane Desalting Buffer (MDB), once again provided with the Kit. To dry the membrane, the column was centrifuged again at 11,000 x g for 1 min. The DNase reaction mixture (10 μ l reconstituted rDNase, 90 μ l Reaction Buffer for rDNase, both provided in the kit) was prepared in a sterile 1.5 ml centrifuge tube and carefully mixed by flicking. 95 μ l of the mixture were added directly onto the middle of the silica membrane and incubated at room temperature for 15 min. The column was placed into a new collection tube. Following incubation, the membrane was washed 3 times. The first wash was done by adding 200 μ l Buffer RAW2 to the column and centrifuging at 11,000 x g for 30 s. The column was then placed into a fresh collection tube. For the second wash, RA3 needed to be prepared, following their specifications. 600 μ l RAW3 were added to the column. After centrifugation at 11,000 x g for 30 s, the column was placed into a new collection tube. For the third wash, another 250 μ l of Buffer RA3 were added to the column. To completely dry the membrane after the wash, centrifugation lasted for 2 min at 11,000 x g. Following this, the column with a dried silica membrane was placed onto a nuclease-free collection tube (part of the kit). The RNA was eluted out of the membrane by adding 60 μ l RNase-free H₂O onto the membrane followed by centrifugation for 2 min at 11,000 x g. After the final centrifugation, the RNA was stored at -80 °C.

4.21. Gene transcription analysis; cDNA synthesis

To perform cDNA synthesis, the exact concentration of mRNA needed to be determined first. We used Nano Drop 2000 for photometric measurement. After two measurements, the mean value of the determined concentration was calculated.

For cDNA synthesis, 1 μ g of RNA in 11 μ l of RNase free water was vortexed. The mixture was then heated to 70 °C. After 5 min, the c-DNA synthesis mix (4 μ l 5xBuffer, 2 μ l Deoxynucleotide Triphosphates, 1 μ l random hexamer RNA Primer, 1 μ l of reverse transcriptase enhancer and 1 μ l of Verso Enzyme mix) was added and the mixture incubated at 42 °C for 1 h (cDNA synthesis), followed by 2 min at 95 °C (inactivation). 30 ml of RNase free water were added to reach a total volume of 50 μ l of diluted cDNA for further experiments. The samples were stored at -20 °C.

4.22. Gene transcription analysis; Quantitative polymerase chain reaction (qPCR)

qPCR functions by monitoring fluorescent signals generated during DNA amplification with modified nucleotides. We used a 384-well plate for detection. Therefore, 2 μ l of diluted c-DNA (1:10), 5 μ l of SYBR Green, 2 μ l of RNase free water and 0.5 μ l of Primer up as well as 0.5 μ l Primer down for the respective mRNA were put in each well, for a total of 10 μ l. PCR synthesis followed the temperature profile described [Table 11: temperature profile qPCR]. We used *CFX384™ Real Time System* to perform the qPCR and the *CFX Manager™* software was used for visualization.

[Table 11: **temperature profile qPCR**]

Function	Temperature [°C]	Time [seconds]
Heating	50	120
Hot start of the Taq Polymerase	95	600
Denaturation	95	10
Primer annealing	55	20
DNA synthesis	72	20

5. Results

5.1. Influence of TMZ on LN229 cells

5.1.1. Cell-cycle distribution, senescence induction and clonogenic survival after treatment of LN229 cells with TMZ

Firstly, the impact of TMZ on cell death and senescence was analysed to verify the results previously observed in this cell system. Flow cytometry was used to determine time-dependent cell death and cell cycle distribution of LN229 cells upon TMZ exposure. The percentage of cells in Sub G1, as indication of dead cells, remained relatively constant among treated cultures [Figure 2, a]. With increasing TMZ dosage, the proportion of cells in G2 and >2n state of the cell cycle showed an increase, while between 50 μM and 100 μM there was no significant change. G2 and >2n cells are associated with senescence, therefore indicating senescence is the dominant result of TMZ treatment [Figure 2, b].

To verify senescence induction by TMZ, treated cells were checked for β -Galactosidase activity as determined by their blue stain under the microscope. All cells treated with TMZ showed a higher degree of β -Galactosidase positive cells compared to the control. In general, a higher dose of TMZ induced a larger portion of x-gal converting cells. Between 50 μM and 100 μM , when accounting for standard deviation, no meaningful increase in the percentage of stained cells was observed. For a treatment of 50 μM of TMZ, the amount most often used in the experiments in this work, roughly 58 % of cells stained blue [Figure 3].

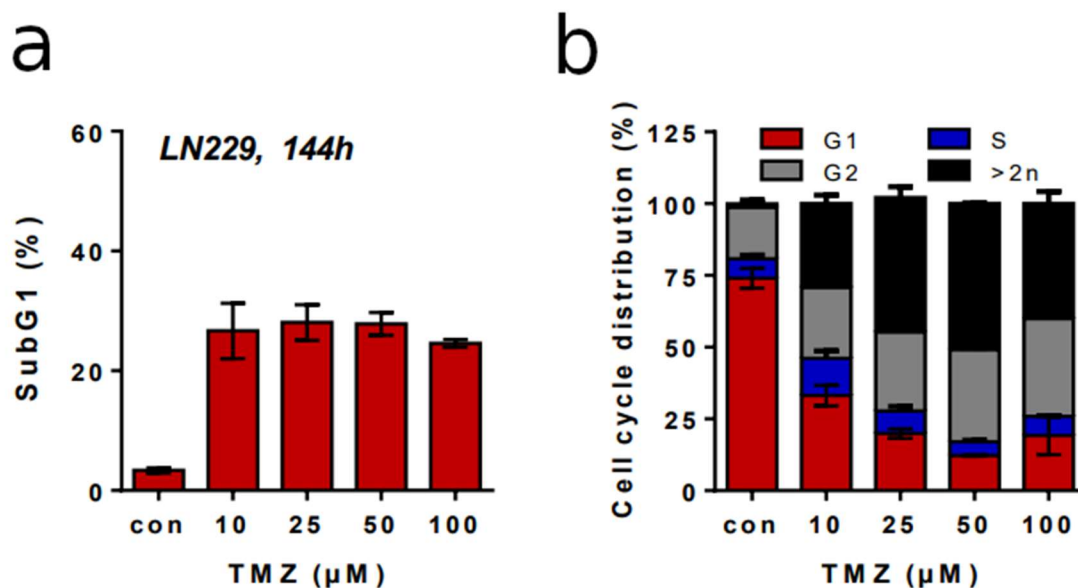


Figure 2: Dose response of LN229 cells after treatment with TMZ. SubG1 and Cell cycle distribution after treatment with TMZ. 144 hours after initial treatment, LN229 cells were harvested and SubG1 fraction (a) and cell cycle distribution (b) were analysed by flow cytometry on BD FACS canto II. GraphPad Prism 6 was used for visualisation.

To analyse colony forming potential of treated cells, colonies grown in the colony forming assays were counted. For the purpose of comparison, the control was set as 100 % colony formation; all treated cell cultures checked for colony formation were set in relation to the control. At a concentration of 50 μM , no viable colonies were detected with an increasing decrease of viable colonies in relation to dosage [Figure 4].

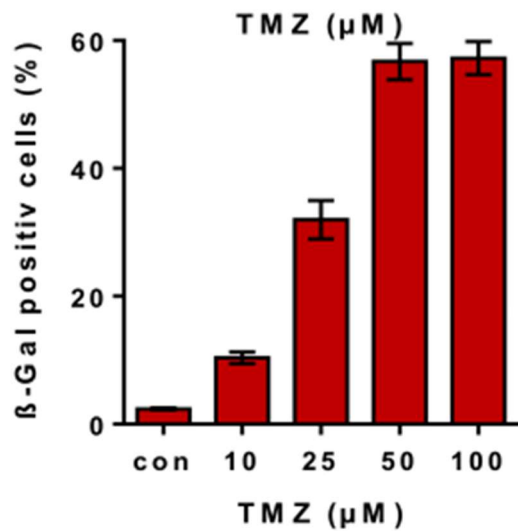


Figure 3: β-Galactosidase assay of LN229 cells after Treatment with TMZ. 120 hours after treatment, LN229 cells were fixed and stained. Pictures were taken by ECHO Rebel microscope camera (magnification ×20), measuring bar: 140 μm.

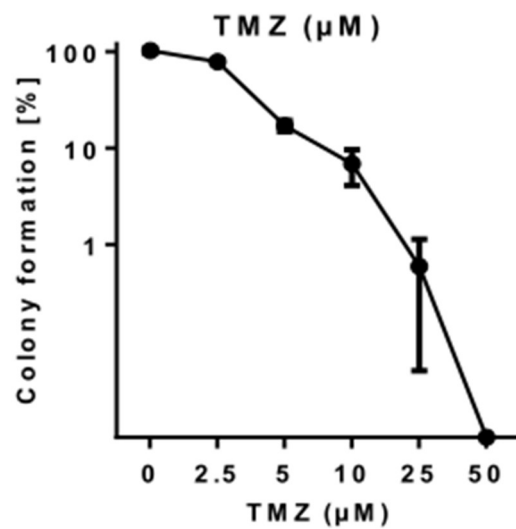


Figure 4: Colony forming assay: Colony formation of LN229 cells after Treatment with TMZ. After treatment, the cells were seeded, and colony formation capability was analysed.

Alltogether, the experiments the experiments show that 50μM TMZ causes only limited cell death, but efficiently arrests cell in the G2/M phase of the cell cycle and induces senescence and a complete block of clonogenic growth, thereby verifying previous results of the Christmann group.

5.1.2. Gene expression analysis after treatment on LN229 cells with TMZ

After successfully verifying previous results concerning senescence induction, qPCR was used to analyse changes to the transcriptome of LN229 cells under TMZ treatment. We choose genes associated with inflammation and senescence associated secretory phenotype, as well as genes with relation to cell cycle and DNA repair. Treatment of LN229 cells with TMZ resulted in a general up regulation in transcription for CCL2, CXCL1, IL6, IL8, CCNA2, CENPF, p21, E2F1, EXO1, FANCI and HMGB1. FOXM1 together with MYBL2 also showed increased expression [Figure 5]. A general decrease in expression under treatment was observed in CCND2, FANCC and FANF [Figure 6]. For IL1A and IL1B, while expression was decreased at the 96 hours' time point, at 144 hours expression was higher than control. For CCNA1, an increase in signal was seen at 144 hours, while at 96 hours showed no significant difference to the control [Figure 6].

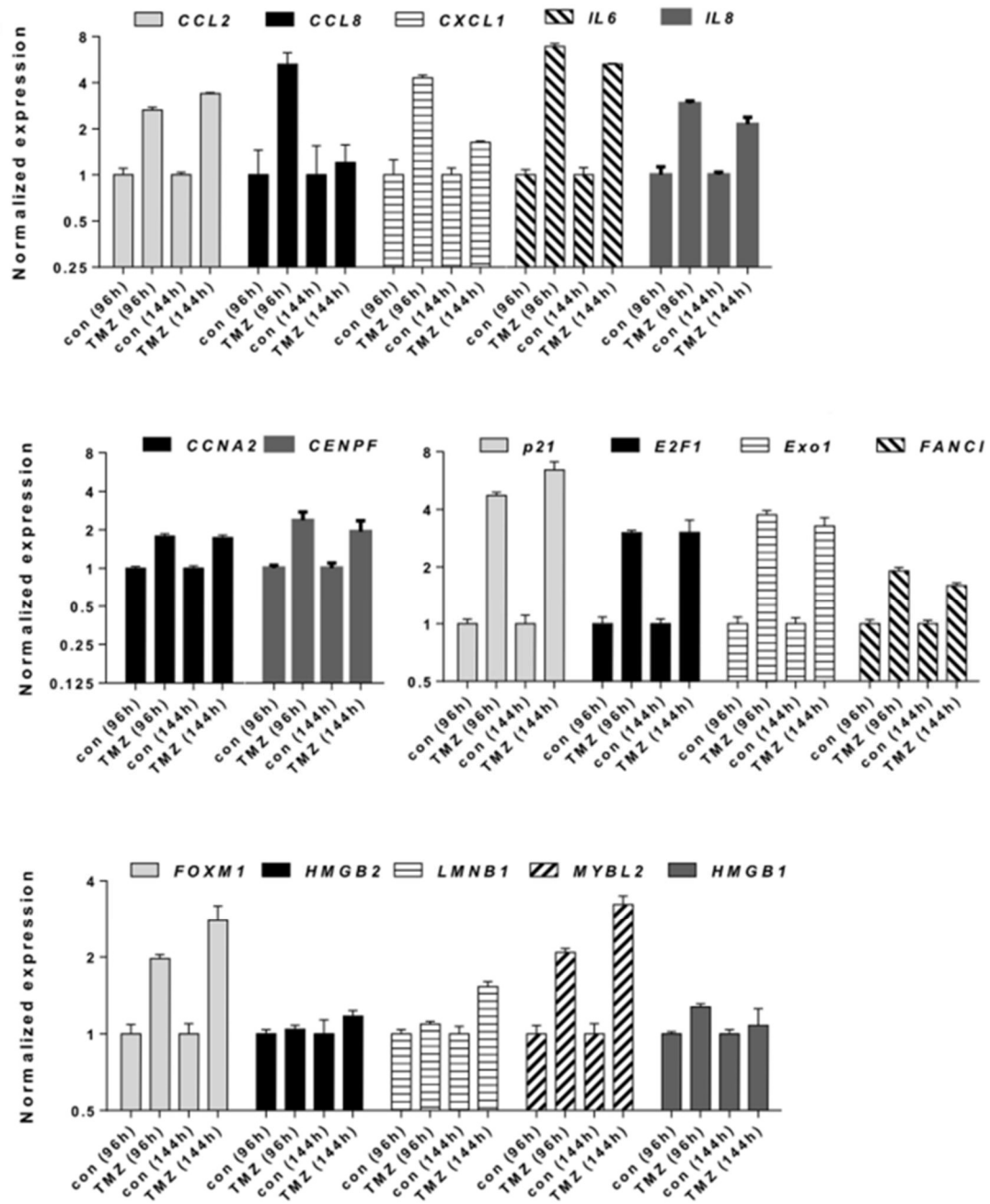


Figure 5: Quantitative qPCR evaluation of CCL2, CCL8, CXCL1, IL6, IL8, CCNA2, CENPF, p21, E2F1, EXO1, FANCI, FOXM1 HMGB1, HMGB2, LMNB1, MYBL2 after TMZ treatment. LN229 cells were treated with 50 μ M 24 hours after seeding and harvested after 96 hours and 144 hours respectively. β -actin and GAPDH were used as reference. The analysis was performed using BioRad CFX Manager™. Graph Prism 6 was used to visualise the data.

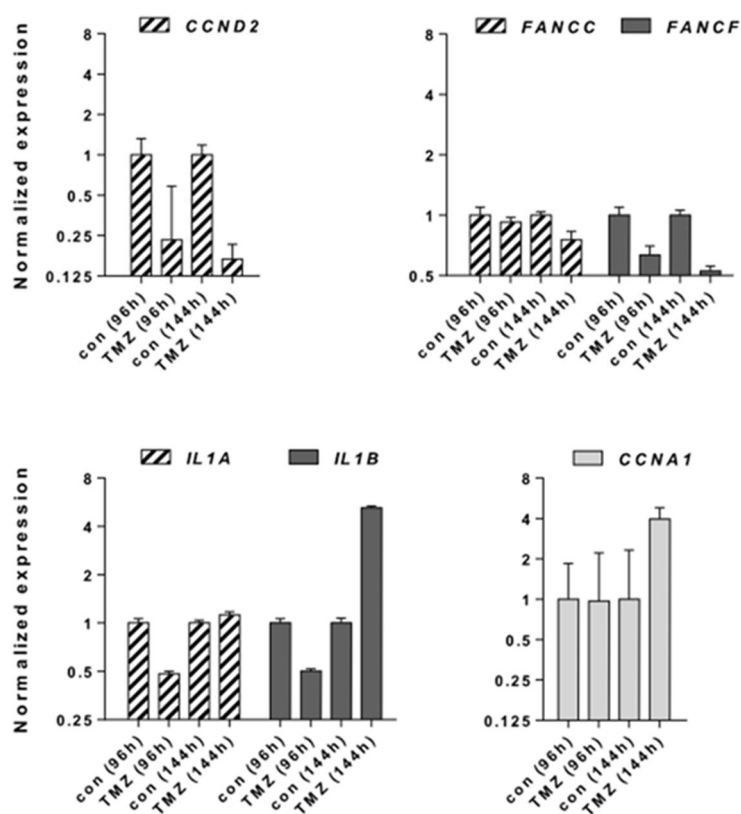


Figure 6: **Quantitative qPCR evaluation of *CCND2*, *FANCC*, *FANCF*, *IL1A*, *IL1B* and *CCNA1* after TMZ treatment.** LN229 cells were treated with 50 μ M 24 hours after seeding and harvested after 96 hours and 144 hours respectively. β -actin and GAPDH were used as reference. The analysis was performed using BioRad CFX Manager™. GraphPad Prism 6 was used to visualise the data.

5.1.3. Protein expression analysis after treatment of LN229 cells with TMZ

Protein expression after TMZ treatment was analysed using immunodetection. TP53INP1 and p21, both associated with cellular senescence, showed an increase in expression. Of proteins associated with cell cycle progression, p130 (a part of the DREAM complex) and BMYB showed a general decrease in expression, while E2F Transcription Factor 5 (E2F5) showed a slight decrease at 96 hours. On the other hand, LIN9 (part of the MUVB complex), E2F Transcription Factor 4 (E2F4) (another part of the DREAM complex) and E2F Transcription Factor 1 (E2F1) showed no significant change in expression, while FOXM1 showed a strongly enhanced expression, concurrent with qPCR analysis. CyclinD1 showed an increase in treated cells at 144 hours [Figure 7].

HMGB1 and HMGB2 showed a decreased expression in treated cells at all time points investigated. LMNB1 and β -catenin showed no significant difference between treated cells and control for all time points investigated [Figure 7].

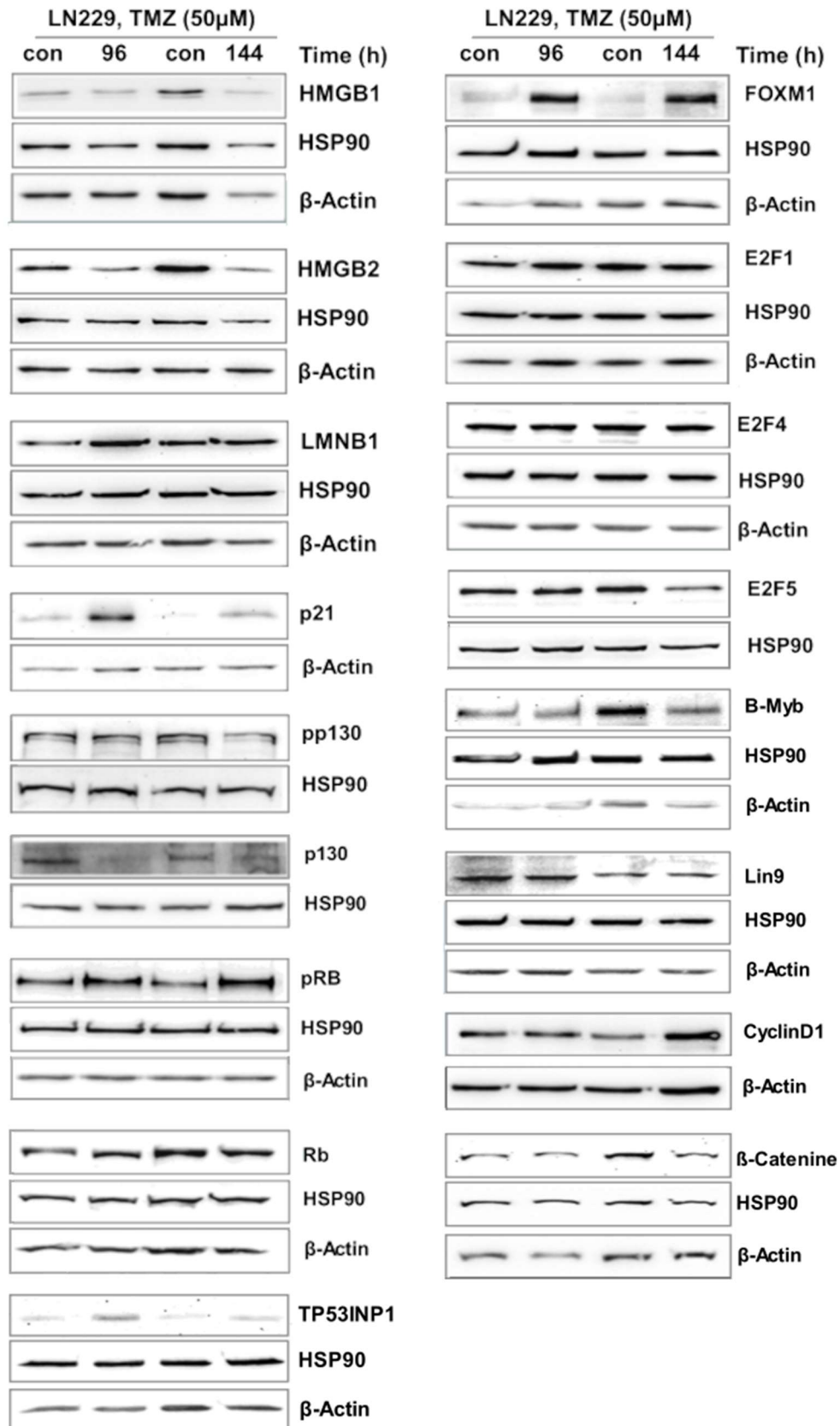


Figure 7: Western transfer analysis of LN229 cells after treatment with TMZ. Cells were treated with 50 μM TMZ 24 hours after seeding. They were harvested after 96 hours and 144 hours respectively. β-Catenin and HSP90 were used for loading control. The iBright CL1000 detection system was used for visualisation. Control (con); 96 and 144 represent timepoints of harvest for respective treated cells.

5.1.4. β -Catenin expression after Treatment of LN229 cells with TMZ and MG132 proteasome inhibition

In addition to factors directly involved in senescence and cell cycle distribution, we also analysed a potential regulation of β -Catenin, which represents an important transcription factor and central player of the β -Catenin/Wnt pathway, which is involved in tumorigenesis and proliferation. β -Catenin expression was analysed 24, 48 and 72 h after TMZ exposure on the protein level using immunodetection. A slight increase in expression of the protein was observed at 24 hours for treated cells, whereas at 48 hours and 72 hours after treatment, β Catenin decreased [Figure 8].

To analyse whether the decrease in β -Catenin is caused by proteasomal degradation, we utilized MG132, an inhibitor of the proteasome. When cells were treated with MG132, the overall expression of β -catenin decreased in accordance to the concentration of MG132. When comparing cells treated with TMZ in addition to MG132 with cells only treated with MG132, no significant change was detected at 96 hours. [Figure 9].

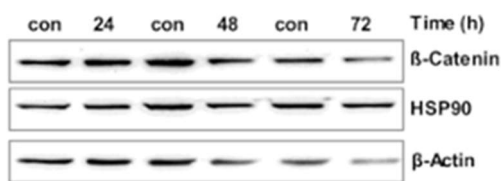


Figure 8: **Western transfer analysis for β -catenin on earlier timepoints.** Cells were treated with 50 μ M TMZ 24 hours after seeding, and harvested at 24 hours, 48 hours and 72 hours respectively.

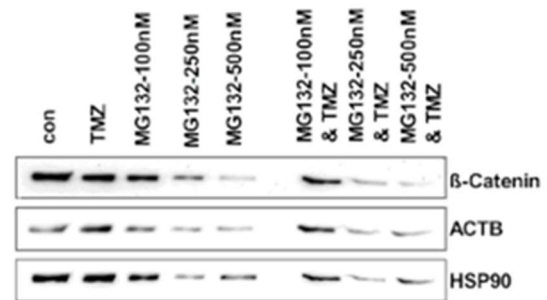


Figure 9: **Western transfer analysis for β -catenin with MG132 inhibition.** Cells were treated with 50 μ M TMZ and MG132 24 hours after seeding and harvested at 96 hours.

6. Discussion

TMZ induces senescence in LN229 glioblastoma cells, as well as autophagy, apoptosis, and necrosis [59]. However overall survival for patients with glioblastoma remains grim even if the tumour responds well to treatment. Working towards a better understanding of the tumour and the treatment-induced phenotype on cellular and molecular level to improve therapeutic outcome for patients as well as treatment is an ongoing effort.

6.1. Chemotherapy with Temozolomide

Currently, the most prominent prognostic factor concerning survival of glioblastoma patients treated with Temozolomide (TMZ) is the grade of methylation of the O⁶-methylguanin-DNA-methyltransferase (MGMT) -promotor [50]. It should be mentioned that The Cancer Genome Atlas (TCGA) Research Network has suggested, MGMT-promotor methylation may only be a relevant biomarker for patient survival when looking at glioblastoma of the classical subtype [61].

LN229 cells are MGMT-deficient and have been shown to be sensitive to TMZ. They express p21 but show no p14/ p16 mRNA expression because of a deletion in the first exon of CDKN2A. The LN229 model resembles classical MGMT-promotor methylated glioblastoma concerning DNA-damage/ DNA-modifications caused by treatment with TMZ.

Experiments, both in this project and other projects of our group as well have shown that after treatment with TMZ, senescence is a major endpoint for MGMT deficient cells such as LN229, mostly dependant on O⁶-methylguanin (O⁶-MeG) above all other DNA adducts caused by TMZ [46]. Our group was further able to show that O⁶-MeG-induced senescence is mediated by via the MRN-ATR pathway, while maintenance of the senescent state is dependent on NF-κB in the absence of p14/p16 [14].

TMZ passes the blood-brain barrier unhindered, and there are no transporters involved that may be dose limiting. In addition to that, due to a more permeable blood-brain barrier, the concentrations in the peritumoral region are likely to be higher compared to the rest of the brain [76]. Peritumoral concentration of the drug varies between studies, partially explained by different treatment plans/schedules. For a rough orientation, Portnow et al 2010 [77], investigated peritumoral concentration after a single dose of TMZ at 150 mg/ m², at least 24 hours after surgery (either debulking craniotomy or stereotactic brain biopsy). *Via* an inserted catheter, measurements of TMZ concentration for the peritumoral region (in this case within 5 mm of the resection cavity) were taken. On average, the peak plasma concentration was 28.4 μM and the peak peritumoral brain interstitium concentration was 3.2 μM. Rosso *et al.*, 2009 [76], using Positron emission tomography-based methods, recorded 14.9–34.5 μM TMZ in the peritumoral region after treatment with 75-200 mg/m². When taking this data together, a concentration of between 3 to 35 μM TMZ are likely, highly dependent upon the dosing regimen used. *In vitro*, concentrations in that span have been shown to induce senescence in a large fraction of the treated MGMT-deficient cells, as seen in our own results [see Figure 8].

In the following pages I will discuss our findings regarding TMZ induced senescence in LN229 cells in more detail.

6.2. TMZ induces senescence and polyploidy in LN229 cells

The flow cytometry of treated LN229 cells showed an increase of cells in G2, as well as an increased amount of polyploid cells. Precious studies of our group have shown that senescence induced by TMZ arrests cells primarily in the G2-M phase of cell cycle progression [14]. Polyploidy is a common characteristic of senescence [60].

Treatment with TMZ also induced an increased percentage of sub-G1 cells correlating with dosage. Sub-G1 describes cells with a degraded or diminished total DNA amount, that tend to be small or fragmented – all hallmarks of apoptotic cells [78]. In our experiments, fewer cells experienced cell death than underwent senescence.

Senescence induced by TMZ was further investigated using a β -Galactosidase assay. At a dose of 50 μ M TMZ, close to 60% of cells stained blue with 5,5`dibromo-4,4`-dichloro-indigo, an indication of their senescence. These results concur with prior research from our group [65] and show that LN229 cells undergo senescence and apoptosis when treated with TMZ. While it is unlikely that a therapeutic setting will achieve a consistent peritumoral concentration around 50 μ M TMZ, treating cells at this concentration does allow for a high percentage of senescent cells for further analysis and research. However, we should state that it is well known that the resistance of tumours cells ex vivo is strongly increased compared to the situation within a tumour, and therefore higher concentrations of a given antitumour drug has to be used in experimental approaches.

6.3. Important changes in the transcriptome

Treatment with TMZ increases expression of forkhead box protein M1 in LN229 cells at both 96 and 144 hours and increases forkhead box protein M1 associated DNA Damage Response gen EXO1 transcription.

Our Western blot analysis showed forkhead box protein M1 (FOXM1) to be increased in expression in senescence, as well as in transcriptome analysis- in both cases at 96 hours as well as 144 hours after treatment. FOXM1 is a member of the forkhead box superfamily of transcription factors. It is pleiotropic in its functions and should be looked at in more detail here.

The FOXM1-gen contains 10 exons, and is alternatively spliced into one of four isoforms; FOXM1a, FOXM1b, FOXM1c and FOXM1d. FOXM1a lacks a transactivation activity and carries both extra exons, Va and VIIa, effectively blocking its transcriptionally active domain. FOXM1b (lacking both exons), FOXM1c (containing Va) and FOXM1d (containing VIIa) are transcriptionally active. FOXM1 in its varying isoforms is known to be upregulated in multiple other solid tumours [79].

In the case of glioblastoma, but not in the normal brain tissue, the main isoform of FOXM1 expressed is FOXM1b [71]. Liu et al., 2006 also showed, that forcing an expression of FOXM1 in anaplastic astrocytoma led to the induction of matrix metalloproteinase-2 (MMP2) and the adoption of an invasive phenotype, comparable to that of glioblastoma, in the brains of mice [40].

In normal cells, FOXM1 plays an important part in cell cycle progression- specifically in G1–S and G2–M cell cycle phase progression. It induces, among others, accumulation of cyclin B1 and cyclin D1 [66,80]. Furthermore, there are consensus sequences for FOXM1 in genomic regions targeted by B-Myb and Lin9; more specifically regions targeted during G2 and mitosis,

meaning these regions are likely to be targets of the B-Myb/MUVB complex, when it recruits FOXM1 during G2 and M phase [81]. Knock-down of FOXM1 even induces senescence in some gastric tumour cells [82] and safeguards the mitotic spindle integrity as well, as its loss leads to mitotic catastrophe [83]. FOXM1 plays a role in reactive oxygen species (ROS) exposed cells, as catalase and superoxide dismutase have been shown to be direct target genes of FOXM1 induced transcription [67]. Further regarding ROS and cell cycle progression under oxidative stress, Anders et al. [68] identified FOXM1 as a target for cyclin D- cyclin dependent- kinase 4/6 phosphorylation, stabilising the transcription factor and thus inducing transcription of FOXM1 target genes. This decreases the amount of ROS, maintenance expression of G1/S phase proteins and even delays senescence. Lastly, FOXM1 drives the transcription for DNA Damage Response (DDR) associated genes; DNA damage sensors, signalling mediators and effectors, such as exonuclease 1 (EXO1) [84].

Nu Zhang et al. 2018 [85] showed, that canonical Wnt activation leads to nuclear accumulation of FOXM1 and β -catenin, with FOXM1 being essential for β -catenin nuclear accumulation, as well as β -catenin/T-cell factor mediated transcription (Hs683 and SW1783 cells were used). β -catenin is often overexpressed in astrocytoma, the lower grade of malignancy to glioblastoma. Its expression increases in correlation with WHO grade, and as such correlates with worsening prognosis [86,87].

β -catenin is dependent on FOXM1 for its nuclear localisation in the case of canonical Wnt-signaling [85]. However, it showed no correlating increase in its expression in our experiments, instead decreasing in treated cells beyond 24 hours [Figure 8]. Since part of the Wnt-signaling change is the inhibition of β -catenin ubiquitination, we would suspect an increase, or at least comparable protein expression to the control. The use of the proteasome inhibitor MG132 caused no significant change in concentration either. A continuous Wnt-signalling and therefore an increase in FOXM1 as part of Wnt-signalling seems further unlikely- at least in so far that no vital, colony forming cells could be observed at 50 μ M TMZ. The increased expression of FOXM1 in our experiment may have been caused by a variety of factors, but it did not result in a reversal of cell cycle arrest.

Xiansheng et al., 2021 [88] have shown an increase in FOXM1 in a concentration dependant relation to ROS induced by H₂O₂. The same project showed evidence of NADPH oxidase 4 derived ROS were involved in FOXM1 induction. Both senescence and the Senescence-associated secretory phenotype (SASP) are typically associated with generation of ROS [89], so a ROS mediated FOXM1 induction is possible. If ROS induce FOXM1 in LN229 cells by directly facilitating enzymatic interaction or indirectly via DNA damage and subsequent DDR, cannot be said for certain at this point. However, DDR signals like p53 have been shown to repress FOXM1 expression in H24 and MCF7-24 cell [69]. Further concerning both p53 in epirubicin treated MCF7 cells, loss of FOXM1 suppression by p53 was associated with drug resistance [70]. LN229 cells used in our experiment express p53 and ATM and both proteins are necessary for the induction of senescence by TMZ treatment [14]. Still, at 98 hours (as well as later time points) FOXM1 still showed a significant increase in our results. If we look at other results presented by our group [90], MCF7 cells treated with Benzo[a]pyren, treated cells showed a decrease in FOXM1 expression over all timepoints investigated, including 96 and 144 hours.

Senescence is associated with continuous DDR signalling [91]. DDR, in the case of TMZ induced DNA damage, will primarily be caused by DSB, dependant on ATR and CHK1 pathways activating p53 as well as ultimately p21 [14]. DSB occur downstream as a consequence of O⁶-MeG, that

cannot be repaired in LN229 cells due to a lack of MGMT. Our group has previously been able to confirm, that DSB remain in senescent cells for long periods of time (at least 10 days) [92]. The total amount of DSB associated signals in a senescent cell culture may decrease over time when looking at the whole, however this likely involves the most severely damaged cells dying [86]. This implies the DNA damage itself is not being rectified - an assumption that coincides with our own groups previous findings concerning DNA repair in TMZ treated cells [14]. Taken together, these findings imply no significant amount of DNA damage is repair taking place in senescent cells, even long into stable senescence while DDR signalling continues. DNA damage of course is not unique to therapy with TMZ. This leaves the type of cell and its specific characteristics as a likely reason for the increase in expression. LN229 cells lack expression of MGMT as well as p14 and p16 [6]. FOXM1 expression is not suppressed in treated cells in our experiment. A p14 / p16 dependent maintenance of FOXM1 repression during senescence may be possible.

FOXM1 however is known to induce transcription of several DNA repair associated genes. Cells treated with cisplatin or doxycycline respectively showed an increased expression of FOXM1, while a knockdown of FOXM1 in turn further sensitises (non-senescent) cells to treatment [93, 94]. In the case of Zhou et al. 2014, the *EXO1* promotor specifically was identified as a strong target for FOXM1 transcription induction, among other genes also responsible for DSB repair such as *BRCA2*, *XRCC1*, *RAD51*, *PLK4* [94]. *EXO1* amplification on an mRNA level is concurrent with our own results for senescent LN229 cells, meaning FOXM1 is likely to be- at least in part- in the nuclei of senescent LN229 cells and shaping transcriptional activity. To verify this, further research needs to be conducted.

Our own group previously described the effect TMZ induced senescence has on DNA repair, for *EXO1* specifically at 24 hours, 48 hours, and 72 hours [14]. Most significantly for the current discussion, TMZ induced senescence coincided with a transcriptional suppression of the mismatch repair genes *MSH2*, *MSH6* and *EXO1*. The results of the project primarily discussed here show *EXO1* mRNA increased at 96 hours and 144 hours after treatment. This implies transcriptional suppression of the DNA damage repair gene *EXO1* on the mRNA level is transitory; it seems to resume at some point after induction of senescence. So far it seems unlikely, that LN229 cells revert to a state of functional DNA repair during senescence induced by TMZ- at least at the concentrations of TMZ used for the treatment in most our experiments here. p21 shows a dynamic of increase and decrease on the protein level [92]- relating to the concept of p21 being essential for senescence induction, not necessarily for continuation or maintenance. p21 mRNA remained strongly expressed in treated cells at both 96 hours and 144 hours however, with 144 hours showing an even greater transcriptional activity. The relationship between mRNA signal and protein decrease indicates a secondary mechanism regulating p21 expression, perhaps by degradation.

While FOXM1 is generally not released outside of the cell, FOXM1 does stimulates the secretion of different proteins into the extracellular spaces. In essence, it is contributing to the SASP, shaping the tumour microenvironment. As a relevant example, FOXM1 increases invasion and angiogenesis in SW1783 and U-87MG glioblastoma cancer cells through induction of matrix metalloproteinase genes *MMP-2* [40]; however as to how many of these cells were senescent is unknown. Therefore, both FOXM1 and Interleukin 6 (see above) are associated with an increased expression of Matrix-Metalloproteinase 2 (*MMP-2*) [39]. Concerning patients with glioblastoma, Matrix-Metalloproteinase 9 (*MMP-9*) has been shown to be inversely correlated to survival as well [95], but Dai B. *et al.*, 2007 was unable to show that FOXM1 induces increased *MMP-9* expression [40]. As stated before, senescent GBM146 and GBM 157 cells

secrete VEGF-A and -C [32], increasing angiogenesis. VEGF are also induced by anoxia in glioblastoma cells. Bevacizumab, an anti-VEGF antibody that lowers angiogenesis, also influences progression-free survival (though not overall survival) [56].

Certainly, these findings show FOXM1, and its targeted genes play a role in the dedifferentiation of malignancies- specifically glioblastoma in this case, further supported by the inverse correlation of FOXM1 overexpression to patient survival [71,96]. Besides an increased expression of FOXM1 in senescent, TMZ treated cells, they did not seem to revert the senescent state, as shown in our colony forming assay. Specifically, the link between SASP and FOXM1 is worth talking about again; both seem to contribute to vascularisation of the tumour and increase its overall invasiveness. While FOXM1 is not part of the SASP, regular overexpression of FOXM1 in some types of glioblastomata or even just individual cells can contribute to shaping the glioblastoma microenvironment into what it is.

FOXM1 should not be looked at without discussing its interaction with the DREAM complex and its individual components. The link between B-MYB and FOXM1 has been subject for studies and reviews before, as well as the connection to the DREAM complex. For one, B-MYB and MuvB are needed to recruit FOXM1 to gene sites in the late G2 phase to facilitate transition to the M- Phase [97]. A knockdown of FOXM1 and BMYB at once (as well as MuvB) with siRNA showed no additive effect on cell division rates [81], implying a common pathway in regular cell cycle progression. Previous studies have managed a stable bypass of senescent human fibroblast cells (CL3EcoR) by inducing a simultaneous expression of all MMB-FOXM1 complex components (MMB consisting of B-Myb/ MYBL2 as well as MUVB) [28].

B-Myb showed a decrease in protein expression in our treated cells. The MUVB protein complex contains Lin9, Lin32, Lin37, Lin54 and RBAP48. In our experiments, Lin9 showed neither a significant decrease nor a significant increase in expression. We did not do a Co-Immunoprecipitation to determine if the MMB complex associates with FOXM1 in senescent cells. It does however seem unlikely that the MMB complex would be functional during senescence, both due to our own results showing the MYBL2 protein component decreased and the fact that inhibition of MYBL2 is commonly associated with senescence [98]. Huang et al., 2010 [57] even showed a MYBL2 dependent suppression of p16 transcription, delaying cell aging and senescence.

It should be noted at this point, that we saw an increase of *MYBL2* transcription in our qPCR [Figure 5]. This is somewhat at odds with first expectations. Other studies using other cell lines tend to show MYBL2 suppression during senescence on both mRNA and protein level [57, 90, 98]. Given MYBL2 and its role in proliferation, it is likely that there are several pathways to control its activity during senescence and an increase in MYBL2 mRNA may be something specific to LN229 cells, as they are lacking p16 expression and subsequently a p16 dependent pathway of senescence induction with its associated transcriptional suppression, other regulatory mechanisms picking up after creation of the mRNA. Our results showed MYBL2 protein to be decreased in senescent cells over all time points investigated, lending further weight to this theory.

Treatment with TMZ does not significantly change expression of E2F transcription factor 1, E2F transcription factor 4 and E2F transcription factor 5

E2F transcription factor 1 (E2F1) is one of the eight members of the E2F family, containing eight members in humans. It remained similarly expressed for all treated cells to the time points

investigated and showed greatly increased mRNA in treated cells at both 96 and 144 hours. E2F1 is a pleiotropic transcription factor, to a likely even greater degree than FOXM1. TMZ has previously shown to disrupt the formation of the E2F1-DP1 complex without necessarily decreasing E2F1 expression [14]. So far it remains unclear just how long said disruption lasts into the senescent state.

The activity of E2F1 is dependent on its dimerization- and binding partners such as dimerization partner (1, 2 or 3), especially during S-phase. Targets of transcription induction are linked to a multitude of cellular mechanisms, including cell proliferation. Once again, our colony forming assay shows a recurrence of mitosis in treated, senescent LN229 cells without further manipulation to be very unlikely. Most interesting for this project however, are the target genes of *MSH2*, *MSH6* and *EXO1*. E2F1 therefore shares *EXO1* as a target gene with FOXM1 and as such the continued suppression of its function after senescence induction can be called into question. To determine if both FOXM1 and E2F1 are necessary to induce *EXO1* expression at later points in senescence or one is sufficient needs to be investigated in further research.

E2F1 has been shown before to both induce a senescence-like phenotype and prevent it. In normal human fibroblasts, so long as p53 was functional, an overexpression resulted in a senescence like state [99]. In the case of the study cited it should be noted, the induction of senescence by E2F1 was shown to be reliant on p14. It has not been reproduced with p14 deficient LN229 cells at the time of writing. On the other hand, E2F1 knockdown has been shown to lead to senescence, and a E2F1 overexpression can suppress senescence associated phenotype, including positive β -Galactosidase staining, in prostate cancer cells (DU145, LNCaP and PC3) treated with Doxorubicin [100].

E2F1 also controls transcription for cell cycle regulated as well as cell cycle regulating genes, such as MYBL2/B-MYB. While B-Myb mRNA showed an increase, on the protein level we found a decrease in expression as already discussed earlier.

E2F transcription factor 4 (E2F4) and E2F transcription factor 5 (E2F5) are both found as part of the DREAM complex. They form their own subgroup in the E2F family and have been generally classified as “repressors”. They generally inhibit the expression of cell cycle genes while they form a complex with RB family proteins, specifically p103 and p130, as part of the DREAM complex [97]. E2F4 showed no significant changes in transcription for the time points investigated. E2F4 is known to play a part in p53 induced, p21 dependent gene suppression [64]- although this does not necessarily lead to senescence, as temporary cell cycle arrest and apoptosis are also possible. It remains to be seen if E2F4 is recruited into a repressor complex and bound to p53 target gene sites during senescence specifically.

We found a slight decrease in E2F5 expression at 144 hours. Generally, E2F5 is very similar to E2F4 and there is little research regarding its role in senescence. The decrease at 144 hours after treatment may therefore be of interest in the future.

p130 and pp130

p130 is part of the DREAM complex. When cells enter the cell cycle, p130 is removed from its association with E2F4/E2F5, releasing cell cycle gene associated promoters from DREAM-dependant suppression. This happens after cyclin D-CDK dependent phosphorylation at tyrosin 410, turning p130 into pp130 [97]. P130 showed a decrease in expression for treated cells, while pp130 showed roughly equal expression in comparison between treated cells and

control. This indicates that the DREAM complex is not assembled during senescence, even though E2F4/E2F5 did not show a significant decrease in expression.

TMZ causes a reduction of high-mobility-group-protein B1 and high-mobility-group-protein B2 expression in treated cells, while increasing mRNA expression for *HMGB1*

Both high-mobility-group-protein B1 (HMGB1) and B2 (HMGB2) are part of the high mobility group of proteins, sequence-nonspecific DNA binding proteins found in vertebrates. The two proteins are fairly homologous, but so far more specific roles for HMGB1 have been described.

In my experiments, treated LN229 cells showed a significant reduction in HMGB1 expression upon treatment, although the control for 144 hours showed a significant increase in comparison to the 96 hours control. HMGB2 expression was decreased on both the protein- and mRNA level. HMGB1 is part of a group of evolutionary highly conserved, non-histone, chromatin-associated proteins and is expressed in almost all eucaryotic cells. It has different functions depending on its localization, post-translational modification, and receptor binding. In its nuclear location, it regulates the transcriptional activity of p53 [101], nuclear factor (NF)- κ B [102], steroid hormone receptors and glucocorticoid receptors [103]. It is also involved in DNA organization / chromatin remodelling, repair and replication [104] and HMGB1 overexpression can be found in most cancer cells, its overexpression being significantly correlated to overall poorer survival of patients [105]. Downregulation of HMGB1 in melanoma cells on the other hand induced the p21 dependent inhibition of cell proliferation, an increase in cell cycle arrest as well as senescence [106].

In addition to its function within the nucleus, HMGB1 has cytokine-like characteristic when secreted into the extracellular space primarily by inflammatory cells [107] or released passively due to cell death- primarily necrosis. When released in such a fashion, it promotes inflammation by increasing local production of tumour-necrosis factor (TNF), interleukin-6 (IL-6) and interferon- γ [108].

The increase in mRNA without corresponding increase on the protein level in our own results are likely at least in part the result of HMGB1 being secreted into the extracellular matrix; both ROS [109] and DNA damage [108] have been shown to induce HMGB1 secretion/release in non-immune cells.

Senescent cells are known to secrete HMGB1 as an important factor of the SASP [110]. Since it is secreted, it does generally does not show up in the proteome we can study with a whole cell extract. Another aspect may be due to it being transported to the nucleus and bound to chromatin much like it has been found with HMGB2 [111], although our protocol for protein extraction should be sufficient to liberate the chaperons from their connection to DNA. HMGB1 in senescent cells showed little nuclear accumulation of HMGB1 in senescent cells, instead active nuclear export can be shown in several different cell lines after they were induced to senescence [110]. Our data is consistent with these results, with decreased HMGB1 protein levels in treated cells.

Much like HMGB1 in its nuclear localization, HMGB2 is involved in transcription, remodelling chromatin to heterochromatin, as well as somatic recombination of lymphocytes. So far, HMGB2 is not considered a cytokine with a function inflammation- unlike HMGB1. However, there is strong evidence to suggest that HMGB2 depletion plays an important role in the induction of senescence, where decrease in HMGB2 expression correlates with extensive chromatin remodelling, even before p21 expression is elevated [112]. Our results concur with

these assumptions.

p21 shows a decrease in expression over time

p21 and its role in TMZ induced senescence has previously been the subject of research, including our group [14]. p21 is the most well-known cyclin-dependent kinase inhibitor and essential to senescence induction and leads to G1, S and G2 cycle arrest as well as senescence in a dose dependent manner [62]. However, p21 is not required for maintenance of senescence and its expression will decrease after the initial burst [62,63], something we can confirm in our findings here. However again, p21 showed a significant increase in mRNA, once more indicating a posttranscriptional process regulating its activity in TMZ treated LN229 cells.

Lamin B1 showed no significant changes in expression in senescent LN229 cells

The nuclear Lamins are the most important structural proteins of the nuclear lamina. This family of proteins contains lamin A, lamin B1, lamin B2 and lamin C. Glia cells, including microglia, generally show low levels of Lamin A/C [113]. Lamin B1 specifically maintains the LA/C and LB2 meshwork found in the lamina, with roughly 75% of lamin B1 deficient cells showing structural abnormalities in the mesh structure. Beyond the nuclear lamina, lamin B1 is also found in the nucleoplasm [114]. It is important for chromatin organisation and transcription [114,115], as well as DNA replication [116] and RNA synthesis [117]. Lamin B1 can bind to regions of the genome close to the nuclear lamina, where it is configured in a repressive chromatin state with reduced transcription [118].

Senescence and especially replicative senescence are associated with a decrease in lamin B1 expression in fibroblasts [119,120]. We did not find a decrease of expression for senescent cells in our experiments.

Barascu et al., 2012 [121] on the other hand found senescence induced by oxidative stress led to an increase in lamin B1 at 3 hours, 6 hours and 9 hours; they also showed that an overexpression of lamin B1 in primary fibroblasts induced senescence. In this case, senescence was induced by oxidative stress. Our results do show an increase in lamin B1 concentration for treated cells at 96 hours, but no significant difference to the control at 144 hours. It seems then, that lamin B1 expression is somewhat dependent on the time point investigated. The behaviour of lamin B1 in LN229 cells during senescence associated with telomere shortening is beyond the scope of this work.

Cyclin D1 showed increased expression in treated cells

Studies have shown a connection between senescence and cyclin D1 [122, 123, 124]. Even though senescent cells can show high concentrations of cyclin D1, they do not show phosphorylation and deactivation of phosphorylated RB and do not enter the S-phase again, even when experiencing mitotic stimuli [122]. In our experiments, the treated cells showed increased expression of cyclin D1, more pronounced for 144 hours than for 96 hours.

6.4. Conclusion

The tumour microenvironment is difficult to gauge from cell models alone; there is no interplay with peripheral immune cells, no vasculature, and no functional microglia mixed in with the malignant cells. All results found in this research apply to at best one of the many cell types found within the heterogenous tumour of a glioblastoma multiforme. Senescent cells in vivo are likely to be forced into their senescence by a multitude of factors, rather than just treatment with TMZ- such as hypoxia, inflammation, irradiation, and oncogene influence.

Still, senescence in LN229 cells shows some peculiarities. FOXM1 expression is not normally associated with senescent cells; looking at the increase in expression in conjunction with the time points investigated in other projects done by our group, a plausible explanation is that FOXM1 repression is dependent/ downstream of p14 or, more likely, p16. These proteins are specifically lacking expression in LN229 cells. The increased transcriptional activity for *MYBL2* and *EXO1* in treated cells may also be a result of that cellular peculiarity and are very likely connected to FOXM1 activity.

So far, it seems FOXM1 expression in senescent cells is not a common occurrence. Further investigation into the suggested p14/p16 dependent pathway of suppression may yield more information. However, FOXM1 activity alone was not enough to revert the senescence like state in our experiments, nor does it seem likely to cause a resumption of DNA repair- at least when looking at the other results by our group. With these characteristic activities of FOXM1 induced transcription blocked by other processes, it may be the case that its increased expression is often simply overlooked.

FOXM1 expression is a known prognostic factor in many cancers, including glioblastoma multiforme. As to what, if any, additional prognostic meaning an increased expression of FOXM1 in glioblastoma- associated senescent cells have, may be difficult to isolate due to the heterogenic population of cells present. However, senescent cells are of especially high interest when it comes to recurrent glioblastoma, as they usually remain in the patient for long times. If FOXM1 is expressed more often than thought so far, especially in long term senescent cells, it most likely plays a role in shaping the environment that allows for a recurrence.

7. Sources and literature

1. Grochans S, Cybulska AM, Simińska D, Korbecki J, Kojder K, Chlubek D, Baranowska-Bosiacka I. Epidemiology of Glioblastoma Multiforme-Literature Review. *Cancers (Basel)*. 2022 May 13;14(10):2412. doi: 10.3390/cancers14102412. PMID: 35626018; PMCID: PMC9139611.
2. Davis ME. Glioblastoma: Overview of Disease and Treatment. *Clin J Oncol Nurs*. 2016 Oct 1;20(5 Suppl):S2-8. doi: 10.1188/16.CJON.S1.2-8. PMID: 27668386; PMCID: PMC5123811.
3. Thakkar JP, Dolecek TA, Horbinski C, Ostrom QT, Lightner DD, Barnholtz-Sloan JS, Villano JL. Epidemiologic and molecular prognostic review of glioblastoma. *Cancer Epidemiol Biomarkers Prev*. 2014 Oct;23(10):1985-96. doi: 10.1158/1055-9965.EPI-14-0275. Epub 2014 Jul 22. PMID: 25053711; PMCID: PMC4185005.
4. Hambardzumyan D, Bergers G. Glioblastoma: Defining Tumor Niches. *Trends Cancer*. 2015 Dec;1(4):252-265. doi: 10.1016/j.trecan.2015.10.009. PMID: 27088132; PMCID: PMC4831073.
5. Prager BC, Bhargava S, Mahadev V, Hubert CG, Rich JN. Glioblastoma Stem Cells: Driving Resilience through Chaos. *Trends Cancer*. 2020 Mar;6(3):223-235. doi: 10.1016/j.trecan.2020.01.009. Epub 2020 Feb 3. PMID: 32101725; PMCID: PMC8779821.
6. LN-229 - CRL-2611 | ATCC [Internet]. www.atcc.org. [cited 2023 February 17.] Available from: <https://www.atcc.org/products/crl-2611>
7. Wu W, Klockow JL, Zhang M, Lafortune F, Chang E, Jin L, Wu Y, Daldrup-Link HE. Glioblastoma multiforme (GBM): An overview of current therapies and mechanisms of resistance. *Pharmacol Res*. 2021 Sep;171:105780. doi: 10.1016/j.phrs.2021.105780. Epub 2021 Jul 21. PMID: 34302977; PMCID: PMC8384724.
8. AWMF Leitlinienregister [Internet]. register.awmf.org. [cited 2022 Feb 26]. Available from: <https://register.awmf.org/de/leitlinien/detail/030-099>. German.
9. Stupp R, Hegi ME, Mason WP, van den Bent MJ, Taphoorn MJ, Janzer RC, Ludwin SK, Allgeier A, Fisher B, Belanger K, Hau P, Brandes AA, Gijtenbeek J, Marosi C, Vecht CJ, Mokhtari K, Wesseling P, Villa S, Eisenhauer E, Gorlia T, Weller M, Lacombe D, Cairncross JG, Mirimanoff RO; European Organisation for Research and Treatment of Cancer Brain Tumour and Radiation Oncology Groups; National Cancer Institute of Canada Clinical Trials Group. Effects of radiotherapy with concomitant and adjuvant temozolomide versus radiotherapy alone on survival in glioblastoma in a randomised phase III study: 5-year analysis of the EORTC-NCIC trial. *Lancet Oncol*. 2009 May;10(5):459-66. doi: 10.1016/S1470-2045(09)70025-7. Epub 2009 Mar 9. PMID: 19269895.
10. Hunter C, Smith R, Cahill DP, Stephens P, Stevens C, Teague J, Greenman C, Edkins S, Bignell G, Davies H, O'Meara S, Parker A, Avis T, Barthorpe S, Brackenbury L, Buck G, Butler A, Clements J, Cole J, Dicks E, Forbes S, Gorton M, Gray K, Halliday K, Harrison R, Hills K, Hinton J, Jenkinson A, Jones D, Kosmidou V, Laman R, Lugg R, Menzies A, Perry J, Petty R, Raine K, Richardson D, Shepherd R, Small A, Solomon H, Tofts C, Varian J, West S, Widaa S, Yates A, Easton DF, Riggins G, Roy JE, Levine KK, Mueller W, Batchelor TT, Louis DN, Stratton MR, Futreal PA, Wooster R. A hypermutation phenotype and somatic MSH6 mutations in recurrent human malignant gliomas after alkylator chemotherapy. *Cancer Res*. 2006 Apr 15;66(8):3987-91. doi: 10.1158/0008-5472.CAN-06-0127. PMID: 16618716; PMCID: PMC7212022.
11. Scudiero DA, Meyer SA, Clatterbuck BE, Mattern MR, Ziolkowski CH, Day RS 3rd. Sensitivity of human cell strains having different abilities to repair O6-methylguanine in DNA to inactivation

- by alkylating agents including chloroethylnitrosoureas. *Cancer Res.* 1984 Jun;44(6):2467-74. PMID: 6722789.
12. Preuss I, Thust R, Kaina B. Protective effect of O6-methylguanine-DNA methyltransferase (MGMT) on the cytotoxic and recombinogenic activity of different antineoplastic drugs. *Int J Cancer.* 1996 Feb 8;65(4):506-12. doi: 10.1002/(SICI)1097-0215(19960208)65:4<506::AID-IJC19>3.0.CO;2-7. PMID: 8621235.
 13. Kondo N, Takahashi A, Ono K, Ohnishi T. DNA damage induced by alkylating agents and repair pathways. *J Nucleic Acids.* 2010 Nov 21;2010:543531. doi: 10.4061/2010/543531. PMID: 21113301; PMCID: PMC2989456.
 14. Aasland D, Göttinger L, Hauck L, Berte N, Meyer J, Effenberger M, Schneider S, Reuber EE, Roos WP, Tomacic MT, Kaina B, Christmann M. Temozolomide Induces Senescence and Repression of DNA Repair Pathways in Glioblastoma Cells via Activation of ATR-CHK1, p21, and NF- κ B. *Cancer Res.* 2019 Jan 1;79(1):99-113. doi: 10.1158/0008-5472.CAN-18-1733. Epub 2018 Oct 25. PMID: 30361254.
 15. Hayflick L, Moorhead Ps. The serial cultivation of human diploid cell strains. *Exp Cell Res.* 1961 Dec;25:585-621. doi: 10.1016/0014-4827(61)90192-6. PMID: 13905658.
 16. Shammas MA. Telomeres, lifestyle, cancer, and aging. *Curr Opin Clin Nutr Metab Care.* 2011 Jan;14(1):28-34. doi: 10.1097/MCO.0b013e32834121b1. PMID: 21102320; PMCID: PMC3370421.
 17. Zhu H, Blake S, Kusuma FK, Pearson RB, Kang J, Chan KT. Oncogene-induced senescence: From biology to therapy. *Mech Ageing Dev.* 2020 Apr;187:111229. doi: 10.1016/j.mad.2020.111229. Epub 2020 Mar 18. PMID: 32171687.
 18. Brack C, Lithgow G, Osiewacz H, Toussaint O. EMBO WORKSHOP REPORT: Molecular and cellular gerontology Serpiano, Switzerland, September 18-22, 1999. *EMBO J.* 2000 May 2;19(9):1929-34. doi: 10.1093/emboj/19.9.1929. PMID: 10790359; PMCID: PMC305699.
 19. Tomari H, Kawamura T, Asanoma K, Egashira K, Kawamura K, Honjo K, Nagata Y, Kato K. Contribution of senescence in human endometrial stromal cells during proliferative phase to embryo receptivity†. *Biol Reprod.* 2020 Jun 23;103(1):104-113. doi: 10.1093/biolre/iaaa044. PMID: 32285109; PMCID: PMC7313258.
 20. Wiley CD, Campisi J. From Ancient Pathways to Aging Cells-Connecting Metabolism and Cellular Senescence. *Cell Metab.* 2016 Jun 14;23(6):1013-1021. doi: 10.1016/j.cmet.2016.05.010. PMID: 27304503; PMCID: PMC4911819.
 21. Passos JF, Nelson G, Wang C, Richter T, Simillion C, Proctor CJ, Miwa S, Olijslagers S, Hallinan J, Wipat A, Saretzki G, Rudolph KL, Kirkwood TB, von Zglinicki T. Feedback between p21 and reactive oxygen production is necessary for cell senescence. *Mol Syst Biol.* 2010;6:347. doi: 10.1038/msb.2010.5. Epub 2010 Feb 16. PMID: 20160708; PMCID: PMC2835567.
 22. Flor AC, Wolfgeher D, Wu D, Kron SJ. A signature of enhanced lipid metabolism, lipid peroxidation and aldehyde stress in therapy-induced senescence. *Cell Death Discov.* 2017 Oct 30;3:17075. doi: 10.1038/cddiscovery.2017.75. PMID: 29090099; PMCID: PMC5661608.

23. Aird KM, Zhang R. Detection of senescence-associated heterochromatin foci (SAHF). *Methods Mol Biol.* 2013;965:185-96. doi: 10.1007/978-1-62703-239-1_12. PMID: 23296659; PMCID: PMC3552318.
24. Hermann G. Ursachen und Folgen zellulärer Seneszenz: Interview mit PD Dr. Gernot Herrmann, Klinik und Poliklinik für Dermatologie und Venerologie, Universität zu Köln [Causes and sequelae of cellular aging: Interview with PD Dr. Gernot Herrmann. *Clinic and Polyclinic of Dermatology and Venereology, Köln University*]. *Hautarzt.* 2006 Nov;57(11):1043-4. German. doi: 10.1007/s00105-006-1254-0. PMID: 17053924. German.
25. Collado M, Gil J, Efeyan A, Guerra C, Schuhmacher AJ, Barradas M, Benguría A, Zaballos A, Flores JM, Barbacid M, Beach D, Serrano M. Tumour biology: senescence in premalignant tumours. *Nature.* 2005 Aug 4;436(7051):642. doi: 10.1038/436642a. PMID: 16079833.
26. Tchkonina T, Zhu Y, van Deursen J, Campisi J, Kirkland JL. Cellular senescence and the senescent secretory phenotype: therapeutic opportunities. *J Clin Invest.* 2013 Mar;123(3):966-72. doi: 10.1172/JCI64098. Epub 2013 Mar 1. PMID: 23454759; PMCID: PMC3582125.
27. Demaria M, Ohtani N, Youssef SA, Rodier F, Toussaint W, Mitchell JR, Laberge RM, Vijg J, Van Steeg H, Dollé ME, Hoeijmakers JH, de Bruin A, Hara E, Campisi J. An essential role for senescent cells in optimal wound healing through secretion of PDGF-AA. *Dev Cell.* 2014 Dec 22;31(6):722-33. doi: 10.1016/j.devcel.2014.11.012. Epub 2014 Dec 11. PMID: 25499914; PMCID: PMC4349629.
28. Kumari R, Hummerich H, Shen X, Fischer M, Litovchick L, Mittnacht S, DeCaprio JA, Jat PS. Simultaneous expression of MMB-FOXM1 complex components enables efficient bypass of senescence. *Sci Rep.* 2021 Nov 2;11(1):21506. doi: 10.1038/s41598-021-01012-z. PMID: 34728711; PMCID: PMC8563780.
29. Dietrich N, Bracken AP, Trinh E, Schjerling CK, Koseki H, Rappsilber J, Helin K, Hansen KH. Bypass of senescence by the polycomb group protein CBX8 through direct binding to the INK4A-ARF locus. *EMBO J.* 2007 Mar 21;26(6):1637-48. doi: 10.1038/sj.emboj.7601632. Epub 2007 Mar 1. PMID: 17332741; PMCID: PMC1829390.
30. Roupakia E, Markopoulos GS, Kolettas E. Genes and pathways involved in senescence bypass identified by functional genetic screens. *Mech Ageing Dev.* 2021 Mar;194:111432. doi: 10.1016/j.mad.2021.111432. Epub 2021 Jan 8. PMID: 33422562.
31. Ouchi R, Okabe S, Migita T, Nakano I, Seimiya H. Senescence from glioma stem cell differentiation promotes tumor growth. *Biochem Biophys Res Commun.* 2016 Feb 5;470(2):275-281. doi: 10.1016/j.bbrc.2016.01.071. Epub 2016 Jan 14. PMID: 26775840; PMCID: PMC5176357.
32. Hinds P, Pietruska J. Senescence and tumor suppression. *F1000Res.* 2017 Dec 11;6:2121. doi: 10.12688/f1000research.11671.1. PMID: 29263785; PMCID: PMC5730862.
33. Lee S, Lee JS. Cellular senescence: a promising strategy for cancer therapy. *BMB Rep.* 2019 Jan;52(1):35-41. doi: 10.5483/BMBRep.2019.52.1.294. PMID: 30526771; PMCID: PMC6386234.
34. Coppé JP, Desprez PY, Krtolica A, Campisi J. The senescence-associated secretory phenotype: the dark side of tumor suppression. *Annu Rev Pathol.* 2010;5:99-118. doi: 10.1146/annurev-pathol-121808-102144. PMID: 20078217; PMCID: PMC4166495.

35. Coppé JP, Patil CK, Rodier F, Sun Y, Muñoz DP, Goldstein J, Nelson PS, Desprez PY, Campisi J. Senescence-associated secretory phenotypes reveal cell-nonautonomous functions of oncogenic RAS and the p53 tumor suppressor. *PLoS Biol.* 2008 Dec 2;6(12):2853-68. doi: 10.1371/journal.pbio.0060301. PMID: 19053174; PMCID: PMC2592359.
36. Weissenberger J, Loeffler S, Kappeler A, Kopf M, Lukes A, Afanasieva TA, Aguzzi A, Weis J. IL-6 is required for glioma development in a mouse model. *Oncogene.* 2004 Apr 22;23(19):3308-16. doi: 10.1038/sj.onc.1207455. PMID: 15064729.
37. Wang H, Lathia JD, Wu Q, Wang J, Li Z, Heddleston JM, Eyler CE, Elderbroom J, Gallagher J, Schuschu J, MacSwords J, Cao Y, McLendon RE, Wang XF, Hjelmeland AB, Rich JN. Targeting interleukin 6 signaling suppresses glioma stem cell survival and tumor growth. *Stem Cells.* 2009 Oct;27(10):2393-404. doi: 10.1002/stem.188. PMID: 19658188; PMCID: PMC2825688.
38. Liu Q, Li G, Li R, Shen J, He Q, Deng L, Zhang C, Zhang J. IL-6 promotion of glioblastoma cell invasion and angiogenesis in U251 and T98G cell lines. *J Neurooncol.* 2010 Nov;100(2):165-76. doi: 10.1007/s11060-010-0158-0. Epub 2010 Apr 2. PMID: 20361349.
39. Li R, Li G, Deng L, Liu Q, Dai J, Shen J, Zhang J. IL-6 augments the invasiveness of U87MG human glioblastoma multiforme cells via up-regulation of MMP-2 and fascin-1. *Oncol Rep.* 2010 Jun;23(6):1553-9. doi: 10.3892/or_00000795. PMID: 20428809.
40. Dai B, Kang SH, Gong W, Liu M, Aldape KD, Sawaya R, Huang S. Aberrant FoxM1B expression increases matrix metalloproteinase-2 transcription and enhances the invasion of glioma cells. *Oncogene.* 2007 Sep 13;26(42):6212-9. doi: 10.1038/sj.onc.1210443. Epub 2007 Apr 2. PMID: 17404569.
41. Brat DJ, Bellail AC, Van Meir EG. The role of interleukin-8 and its receptors in gliomagenesis and tumoral angiogenesis. *Neuro Oncol.* 2005 Apr;7(2):122-33. doi: 10.1215/S1152851704001061. PMID: 15831231; PMCID: PMC1871893.
42. Raychaudhuri B, Vogelbaum MA. IL-8 is a mediator of NF- κ B induced invasion by gliomas. *J Neurooncol.* 2011 Jan;101(2):227-35. doi: 10.1007/s11060-010-0261-2. Epub 2010 Jun 25. PMID: 20577780.
43. Xue H, Yuan G, Guo X, Liu Q, Zhang J, Gao X, Guo X, Xu S, Li T, Shao Q, Yan S, Li G. A novel tumor-promoting mechanism of IL6 and the therapeutic efficacy of tocilizumab: Hypoxia-induced IL6 is a potent autophagy initiator in glioblastoma via the p-STAT3-MIR155-3p-CREBRF pathway. *Autophagy.* 2016 Jul 2;12(7):1129-52. doi: 10.1080/15548627.2016.1178446. Epub 2016 May 10. PMID: 27163161; PMCID: PMC4990999.
44. Desbaillets I, Diserens AC, de Tribolet N, Hamou MF, Van Meir EG. Regulation of interleukin-8 expression by reduced oxygen pressure in human glioblastoma. *Oncogene.* 1999 Feb 18;18(7):1447-56. doi: 10.1038/sj.onc.1202424. PMID: 10050881.
45. Vaupel P. Hypoxia and aggressive tumor phenotype: implications for therapy and prognosis. *Oncologist.* 2008;13 Suppl 3:21-6. doi: 10.1634/theoncologist.13-S3-21. PMID: 18458121.
46. Roos WP, Batista LF, Naumann SC, Wick W, Weller M, Menck CF, Kaina B. Apoptosis in malignant glioma cells triggered by the temozolomide-induced DNA lesion O6-methylguanine. *Oncogene.* 2007 Jan 11;26(2):186-97. doi: 10.1038/sj.onc.1210443. Epub 2007 Apr 2. PMID: 17404569. Roos WP, Batista LF, Naumann SC, Wick W, Weller M, Menck CF, Kaina B. Apoptosis in malignant glioma cells triggered by the temozolomide-

- induced DNA lesion O6-methylguanine. *Oncogene*. 2007 Jan 11;26(2):186-97. doi: 10.1038/sj.onc.1209785. Epub 2006 Jul 3. PMID: 16819506.
47. Kaina B, Christmann M, Naumann S, Roos WP. MGMT: key node in the battle against genotoxicity, carcinogenicity and apoptosis induced by alkylating agents. *DNA Repair (Amst)*. 2007 Aug 1;6(8):1079-99. doi: 10.1016/j.dnarep.2007.03.008. Epub 2007 May 7. PMID: 17485253.
 48. Pegg AE, Roberfroid M, von Bahr C, Foote RS, Mitra S, Bresil H, Likhachev A, Montesano R. Removal of O6-methylguanine from DNA by human liver fractions. *Proc Natl Acad Sci U S A*. 1982 Sep;79(17):5162-5. doi: 10.1073/pnas.79.17.5162. PMID: 6957855; PMCID: PMC346854.
 49. Day RS 3rd, Ziolkowski CH, Scudiero DA, Meyer SA, Lubiniecki AS, Girardi AJ, Galloway SM, Bynum GD. Defective repair of alkylated DNA by human tumour and SV40-transformed human cell strains. *Nature*. 1980 Dec 25;288(5792):724-7. doi: 10.1038/288724a0. PMID: 6256643.
 50. Hegi ME, Diserens AC, Gorlia T, Hamou MF, de Tribolet N, Weller M, Kros JM, Hainfellner JA, Mason W, Mariani L, Bromberg JE, Hau P, Mirimanoff RO, Cairncross JG, Janzer RC, Stupp R. MGMT gene silencing and benefit from temozolomide in glioblastoma. *N Engl J Med*. 2005 Mar 10;352(10):997-1003. doi: 10.1056/NEJMoa043331. PMID: 15758010.
 51. White RR, Milholland B, de Bruin A, Curran S, Laberge RM, van Steeg H, Campisi J, Maslov AY, Vijg J. Controlled induction of DNA double-strand breaks in the mouse liver induces features of tissue ageing. *Nat Commun*. 2015 Apr 10;6:6790. doi: 10.1038/ncomms7790. PMID: 25858675; PMCID: PMC4394211.
 52. Halazonetis TD, Gorgoulis VG, Bartek J. An oncogene-induced DNA damage model for cancer development. *Science*. 2008 Mar 7;319(5868):1352-5. doi: 10.1126/science.1140735. PMID: 18323444. c.1209785. Epub 2006 Jul 3. PMID: 16819506.
 53. Litovchick L, Sadasivam S, Florens L, Zhu X, Swanson SK, Velmurugan S, Chen R, Washburn MP, Liu XS, DeCaprio JA. Evolutionarily conserved multisubunit RBL2/p130 and E2F4 protein complex represses human cell cycle-dependent genes in quiescence. *Mol Cell*. 2007 May 25;26(4):539-51. doi: 10.1016/j.molcel.2007.04.015. PMID: 17531812.
 54. Lefebvre C, Rajbhandari P, Alvarez MJ, Bandaru P, Lim WK, Sato M, Wang K, Sumazin P, Kustagi M, Bisikirska BC, Basso K, Beltrao P, Krogan N, Gautier J, Dalla-Favera R, Califano A. A human B-cell interactome identifies MYB and FOXM1 as master regulators of proliferation in germinal centers. *Mol Syst Biol*. 2010 Jun 8;6:377. doi: 10.1038/msb.2010.31. PMID: 20531406; PMCID: PMC2913282.
 55. Joaquin M, Watson RJ. Cell cycle regulation by the B-Myb transcription factor. *Cell Mol Life Sci*. 2003 Nov;60(11):2389-401. doi: 10.1007/s00018-003-3037-4. PMID: 14625684.
 56. Wu L, Timmers C, Maiti B, Saavedra HI, Sang L, Chong GT, Nuckolls F, Giangrande P, Wright FA, Field SJ, Greenberg ME, Orkin S, Nevins JR, Robinson ML, Leone G. The E2F1-3 transcription factors are essential for cellular proliferation. *Nature*. 2001 Nov 22;414(6862):457-62. doi: 10.1038/35106593. PMID: 11719808
 57. Huang Y, Wu J, Li R, Wang P, Han L, Zhang Z, Tong T. B-MYB delays cell aging by repressing p16 (INK4 α) transcription. *Cell Mol Life Sci*. 2011 Mar;68(5):893-901. doi: 10.1007/s00018-010-0501-9. Epub 2010 Aug 25. PMID: 20734103.

58. Quaas M, Müller GA, Engeland K. p53 can repress transcription of cell cycle genes through a p21(WAF1/CIP1)-dependent switch from MMB to DREAM protein complex binding at CHR promoter elements. *Cell Cycle*. 2012 Dec 15;11(24):4661-72. doi: 10.4161/cc.22917. Epub 2012 Nov 27. PMID: 23187802; PMCID: PMC3562311.
59. Kurz DJ, Decary S, Hong Y, Erusalimsky JD. Senescence-associated (beta)-galactosidase reflects an increase in lysosomal mass during replicative ageing of human endothelial cells. *J Cell Sci*. 2000 Oct;113 (Pt 20):3613-22. doi: 10.1242/jcs.113.20.3613. PMID: 11017877.
60. Sikora E, Bielak-Zmijewska A, Mosieniak G. A common signature of cellular senescence; does it exist? *Ageing Res Rev*. 2021 Nov;71:101458. doi: 10.1016/j.arr.2021.101458. Epub 2021 Sep 6. PMID: 34500043.
61. Brennan CW, Verhaak RG, McKenna A, Campos B, Nouseh H, Salama SR, Zheng S, Chakravarty D, Sanborn JZ, Berman SH, Beroukhi R, Bernard B, Wu CJ, Genovese G, Shmulevich I, Barnholtz-Sloan J, Zou L, Vegesna R, Shukla SA, Ciriello G, Yung WK, Zhang W, Sougnez C, Mikkelsen T, Aldape K, Bigner DD, Van Meir EG, Prados M, Sloan A, Black KL, Eschbacher J, Finocchiaro G, Friedman W, Andrews DW, Guha A, Iacocca M, O'Neill BP, Foltz G, Myers J, Weisenberger DJ, Penny R, Kucherlapati R, Perou CM, Hayes DN, Gibbs R, Marra M, Mills GB, Lander E, Spellman P, Wilson R, Sander C, Weinstein J, Meyerson M, Gabriel S, Laird PW, Haussler D, Getz G, Chin L; TCGA Research Network. The somatic genomic landscape of glioblastoma. *Cell*. 2013 Oct 10;155(2):462-77. doi: 10.1016/j.cell.2013.09.034. Erratum in: *Cell*. 2014 Apr 24;157(3):753. PMID: 24120142; PMCID: PMC3910500.
62. Shtutman M, Chang BD, Schools GP, Broude EV. Cellular Model of p21-Induced Senescence. *Methods Mol Biol*. 2017;1534:31-39. doi: 10.1007/978-1-4939-6670-7_3. PMID: 27812865; PMCID: PMC6764449
63. Stein GH, Drullinger LF, Soulard A, Dulić V. Differential roles for cyclin-dependent kinase inhibitors p21 and p16 in the mechanisms of senescence and differentiation in human fibroblasts. *Mol Cell Biol*. 1999 Mar;19(3):2109-17. doi: 10.1128/MCB.19.3.2109. PMID: 10022898; PMCID: PMC84004.
64. Benson EK, Mungamuri SK, Attie O, Kracikova M, Sachidanandam R, Manfredi JJ, Aaronson SA. p53-dependent gene repression through p21 is mediated by recruitment of E2F4 repression complexes. *Oncogene*. 2014 Jul 24;33(30):3959-69. doi: 10.1038/onc.2013.378. Epub 2013 Oct 7. PMID: 24096481; PMCID: PMC4067464.
65. Beltzig L, Schwarzenbach C, Leukel P, Frauenknecht KBM, Sommer C, Tancredi A, Hegi ME, Christmann M, Kaina B. Senescence Is the Main Trait Induced by Temozolomide in Glioblastoma Cells. *Cancers (Basel)*. 2022 Apr 29;14(9):2233. doi: 10.3390/cancers14092233. PMID: 35565362; PMCID: PMC9102829.
66. Wang X, Quail E, Hung NJ, Tan Y, Ye H, Costa RH. Increased levels of forkhead box M1B transcription factor in transgenic mouse hepatocytes prevent age-related proliferation defects in regenerating liver. *Proc Natl Acad Sci U S A*. 2001 Sep 25;98(20):11468-73. doi: 10.1073/pnas.201360898. PMID: 11572993; PMCID: PMC58753.
67. Park HJ, Carr JR, Wang Z, Nogueira V, Hay N, Tyner AL, Lau LF, Costa RH, Raychaudhuri P. FoxM1, a critical regulator of oxidative stress during oncogenesis. *EMBO J*. 2009 Oct 7;28(19):2908-18. doi: 10.1038/emboj.2009.239. Epub 2009 Aug 20. PMID: 19696738; PMCID: PMC2760115.
68. Anders L, Ke N, Hydbring P, Choi YJ, Widlund HR, Chick JM, Zhai H, Vidal M, Gygi SP, Braun P, Sicinski P. A systematic screen for CDK4/6 substrates links FOXM1 phosphorylation to senescence suppression in cancer cells. *Cancer Cell*. 2011 Nov 15;20(5):620-34. doi: 10.1016/j.ccr.2011.10.001. PMID: 22094256; PMCID: PMC3237683.

69. Barsotti AM, Prives C. Pro-proliferative FoxM1 is a target of p53-mediated repression. *Oncogene*. 2009 Dec 3;28(48):4295-305. doi: 10.1038/onc.2009.282. Epub 2009 Sep 14. PMID: 19749794; PMCID: PMC2898139.
70. Millour J, de Olano N, Horimoto Y, Monteiro LJ, Langer JK, Aligue R, Hajji N, Lam EW. ATM and p53 regulate FOXM1 expression via E2F in breast cancer epirubicin treatment and resistance. *Mol Cancer Ther*. 2011 Jun;10(6):1046-58. doi: 10.1158/1535-7163.MCT-11-0024. Epub 2011 Apr 25. PMID: 21518729; PMCID: PMC4845881.
71. Liu M, Dai B, Kang SH, Ban K, Huang FJ, Lang FF, Aldape KD, Xie TX, Pelloski CE, Xie K, Sawaya R, Huang S. FoxM1B is overexpressed in human glioblastomas and critically regulates the tumorigenicity of glioma cells. *Cancer Res*. 2006 Apr 1;66(7):3593-602. doi: 10.1158/0008-5472.CAN-05-2912. PMID: 16585184.
72. Knizhnik AV, Roos WP, Nikolova T, Quiros S, Tomaszowski KH, Christmann M, Kaina B. Survival and death strategies in glioma cells: autophagy, senescence and apoptosis triggered by a single type of temozolomide-induced DNA damage. *PLoS One*. 2013;8(1):e55665. doi: 10.1371/journal.pone.0055665. Epub 2013 Jan 30. PMID: 23383259; PMCID: PMC3559438.
73. Picot J, Guerin CL, Le Van Kim C, Boulanger CM. Flow cytometry: retrospective, fundamentals and recent instrumentation. *Cytotechnology*. 2012 Mar;64(2):109-30. doi: 10.1007/s10616-011-9415-0. Epub 2012 Jan 21. PMID: 22271369; PMCID: PMC3279584.
74. Kurz DJ, Decary S, Hong Y, Erusalimsky JD. Senescence-associated (beta)-galactosidase reflects an increase in lysosomal mass during replicative ageing of human endothelial cells. *J Cell Sci*. 2000 Oct;113 (Pt 20):3613-22. doi: 10.1242/jcs.113.20.3613. PMID: 11017877.
75. Bradford MM. A rapid and sensitive method for the quantitation of microgram quantities of protein utilizing the principle of protein-dye binding. *Anal Biochem*. 1976 May 7;72:248-54. doi: 10.1006/abio.1976.9999. PMID: 942051.
76. Rosso L, Brock CS, Gallo JM, Saleem A, Price PM, Turkheimer FE, Aboagye EO. A new model for prediction of drug distribution in tumor and normal tissues: pharmacokinetics of temozolomide in glioma patients. *Cancer Res*. 2009 Jan 1;69(1):120-7. doi: 10.1158/0008-5472.CAN-08-2356. PMID: 19117994
77. Portnow J, Badie B, Chen M, Liu A, Blanchard S, Synold TW. The neuropharmacokinetics of temozolomide in patients with resectable brain tumors: potential implications for the current approach to chemoradiation. *Clin Cancer Res*. 2009 Nov 15;15(22):7092-8. doi: 10.1158/1078-0432.CCR-09-1349. Epub 2009 Oct 27. PMID: 19861433; PMCID: PMC2908372.
78. Kajstura M, Halicka HD, Pryjma J, Darzynkiewicz Z. Discontinuous fragmentation of nuclear DNA during apoptosis revealed by discrete "sub-G1" peaks on DNA content histograms. *Cytometry A*. 2007 Mar;71(3):125-31. doi: 10.1002/cyto.a.20357. PMID: 17252584.
79. Pilarsky C, Wenzig M, Specht T, Saeger HD, Grützmann R. Identification and validation of commonly overexpressed genes in solid tumors by comparison of microarray data. *Neoplasia*. 2004 Nov-Dec;6(6):744-50. doi: 10.1593/neo.04277. PMID: 15720800; PMCID: PMC1531678.
80. Leung TW, Lin SS, Tsang AC, Tong CS, Ching JC, Leung WY, Gimlich R, Wong GG, Yao KM. Over-expression of FoxM1 stimulates cyclin B1 expression. *FEBS Lett*. 2001 Oct 19;507(1):59-66. doi: 10.1016/s0014-5793(01)02915-5. PMID: 11682060.
81. Sadasivam S, Duan S, DeCaprio JA. The MuvB complex sequentially recruits B-Myb and FoxM1 to promote mitotic gene expression. *Genes Dev*. 2012 Mar 1;26(5):474-89. doi: 10.1101/gad.181933.111. PMID: 22391450; PMCID: PMC3305985.
82. Zeng J, Wang L, Li Q, Li W, Björkholm M, Jia J, Xu D. FoxM1 is up-regulated in gastric cancer and its inhibition leads to cellular senescence, partially dependent on p27 kip1. *J Pathol*. 2009 Aug;218(4):419-27. doi: 10.1002/path.2530. PMID: 19235838.

83. Wonsey DR, Follettie MT. Loss of the forkhead transcription factor FoxM1 causes centrosome amplification and mitotic catastrophe. *Cancer Res.* 2005 Jun 15;65(12):5181-9. doi: 10.1158/0008-5472.CAN-04-4059. PMID: 15958562.
84. Zona S, Bella L, Burton MJ, Nestal de Moraes G, Lam EW. FOXM1: an emerging master regulator of DNA damage response and genotoxic agent resistance. *Biochim Biophys Acta.* 2014 Nov;1839(11):1316-22. doi: 10.1016/j.bbagr.2014.09.016. Epub 2014 Oct 5. PMID: 25287128; PMCID: PMC4316173.
85. Zhang N, Wei P, Gong A, Chiu WT, Lee HT, Colman H, Huang H, Xue J, Liu M, Wang Y, Sawaya R, Xie K, Yung WK, Medema RH, He X, Huang S. FoxM1 promotes β -catenin nuclear localization and controls Wnt target-gene expression and glioma tumorigenesis. *Cancer Cell.* 2011 Oct 18;20(4):427-42. doi: 10.1016/j.ccr.2011.08.016. PMID: 22014570; PMCID: PMC3199318.
86. Sareddy GR, Panigrahi M, Challa S, Mahadevan A, Babu PP. Activation of Wnt/beta-catenin/Tcf signaling pathway in human astrocytomas. *Neurochem Int.* 2009 Sep;55(5):307-17. doi: 10.1016/j.neuint.2009.03.016. Epub 2009 Apr 5. PMID: 19576519.
87. Liu C, Tu Y, Sun X, Jiang J, Jin X, Bo X, Li Z, Bian A, Wang X, Liu D, Wang Z, Ding L. Wnt/beta-Catenin pathway in human glioma: expression pattern and clinical/prognostic correlations. *Clin Exp Med.* 2011 Jun;11(2):105-12. doi: 10.1007/s10238-010-0110-9. Epub 2010 Aug 31. PMID: 20809334.
88. Su X, Yang Y, Yang Q, Pang B, Sun S, Wang Y, Qiao Q, Guo C, Liu H, Pang Q. NOX4-derived ROS-induced overexpression of FOXM1 regulates aerobic glycolysis in glioblastoma. *BMC Cancer.* 2021 Nov 5;21(1):1181. doi: 10.1186/s12885-021-08933-y. PMID: 34740322; PMCID: PMC8571893.
89. Davalli P, Mitic T, Caporali A, Lauriola A, D'Arca D. ROS, Cell Senescence, and Novel Molecular Mechanisms in Aging and Age-Related Diseases. *Oxid Med Cell Longev.* 2016;2016:3565127. doi: 10.1155/2016/3565127. Epub 2016 May 10. PMID: 27247702; PMCID: PMC4877482.
90. Schmidt A. The role of the DREAM complex and TP53INP1 in B[a]P-induced senescence. Unpublished.
91. Fumagalli M, Rossiello F, Mondello C, d'Adda di Fagagna F. Stable cellular senescence is associated with persistent DDR activation. *PLoS One.* 2014 Oct 23;9(10):e110969. doi: 10.1371/journal.pone.0110969. PMID: 25340529; PMCID: PMC4207795
92. Beltzig L, Stratenwerth B, Kaina B. Accumulation of Temozolomide-Induced Apoptosis, Senescence and DNA Damage by Metronomic Dose Schedule: A Proof-of-Principle Study with Glioblastoma Cells. *Cancers (Basel).* 2021 Dec 14;13(24):6287. doi: 10.3390/cancers13246287. PMID: 34944906; PMCID: PMC8699541.
93. Tan Y, Raychaudhuri P, Costa RH. Chk2 mediates stabilization of the FoxM1 transcription factor to stimulate expression of DNA repair genes. *Mol Cell Biol.* 2007 Feb;27(3):1007-16. doi: 10.1128/MCB.01068-06. Epub 2006 Nov 13. PMID: 17101782; PMCID: PMC1800696.
94. Zhou J, Wang Y, Wang Y, Yin X, He Y, Chen L, Wang W, Liu T, Di W. FOXM1 modulates cisplatin sensitivity by regulating EXO1 in ovarian cancer. *PLoS One.* 2014 May 13;9(5):e96989. doi: 10.1371/journal.pone.0096989. PMID: 24824601; PMCID: PMC4019642.
95. Dobra G, Gyukity-Sebestyén E, Bukva M, Harmati M, Nagy V, Szabó Z, Pankotai T, Klekner Á, Buzás K. MMP-9 as Prognostic Marker for Brain Tumours: A Comparative Study on Serum-Derived Small Extracellular Vesicles. *Cancers (Basel).* 2023 Jan 24;15(3):712. doi: 10.3390/cancers15030712. PMID: 36765669; PMCID: PMC9913777.
96. Wang Z, Zhang S, Siu TL, Huang S. Glioblastoma multiforme formation and EMT: role of FoxM1 transcription factor. *Curr Pharm Des.* 2015;21(10):1268-71. doi: 10.2174/1381612821666141211115949. PMID: 25506897; PMCID: PMC4380124.

97. Sadasivam S, DeCaprio JA. The DREAM complex: master coordinator of cell cycle-dependent gene expression. *Nat Rev Cancer*. 2013 Aug;13(8):585-95. doi: 10.1038/nrc3556. Epub 2013 Jul 11. Erratum in: *Nat Rev Cancer*. 2013 Oct;13(10):752. PMID: 23842645; PMCID: PMC3986830.
98. Zhou Z, Yin Y, Chang Q, Sun G, Lin J, Dai Y. Downregulation of B-myb promotes senescence via the ROS-mediated p53/p21 pathway, in vascular endothelial cells. *Cell Prolif*. 2017 Apr;50(2):e12319. doi: 10.1111/cpr.12319. Epub 2016 Nov 23. PMID: 27878894; PMCID: PMC6529094.
99. Dimri GP, Itahana K, Acosta M, Campisi J. Regulation of a senescence checkpoint response by the E2F1 transcription factor and p14(ARF) tumor suppressor. *Mol Cell Biol*. 2000 Jan;20(1):273-85. doi: 10.1128/MCB.20.1.273-285.2000. PMID: 10594030; PMCID: PMC85083.
100. Park C, Lee I, Kang WK. E2F-1 is a critical modulator of cellular senescence in human cancer. *Int J Mol Med*. 2006 May;17(5):715-20. PMID: 16596252.
101. Rowell JP, Simpson KL, Stott K, Watson M, Thomas JO. HMGB1-facilitated p53 DNA binding occurs via HMG-Box/p53 transactivation domain interaction, regulated by the acidic tail. *Structure*. 2012 Dec 5;20(12):2014-24. doi: 10.1016/j.str.2012.09.004. Epub 2012 Oct 11. PMID: 23063560
102. Luan ZG, Zhang H, Yang PT, Ma XC, Zhang C, Guo RX. HMGB1 activates nuclear factor- κ B signaling by RAGE and increases the production of TNF- α in human umbilical vein endothelial cells. *Immunobiology*. 2010 Dec;215(12):956-62. doi: 10.1016/j.imbio.2009.11.001. Epub 2010 Feb 18. PMID: 20163887.
103. Verrijdt G, Haelens A, Schoenmakers E, Rombauts W, Claessens F. Comparative analysis of the influence of the high-mobility group box 1 protein on DNA binding and transcriptional activation by the androgen, glucocorticoid, progesterone and mineralocorticoid receptors. *Biochem J*. 2002 Jan 1;361(Pt 1):97-103. doi: 10.1042/0264-6021:3610097. PMID: 11742533; PMCID: PMC1222283.
104. Stros M. HMGB proteins: interactions with DNA and chromatin. *Biochim Biophys Acta*. 2010 Jan-Feb;1799(1-2):101-13. doi: 10.1016/j.bbagr.2009.09.008. PMID: 20123072.
105. Wu T, Zhang W, Yang G, Li H, Chen Q, Song R, Zhao L. HMGB1 overexpression as a prognostic factor for survival in cancer: a meta-analysis and systematic review. *Oncotarget*. 2016 Aug 2;7(31):50417-50427. doi: 10.18632/oncotarget.10413. PMID: 27391431; PMCID: PMC5226592.
106. Li Q, Li J, Wen T, Zeng W, Peng C, Yan S, Tan J, Yang K, Liu S, Guo A, Zhang C, Su J, Jiang M, Liu Z, Zhou H, Chen X. Overexpression of HMGB1 in melanoma predicts patient survival and suppression of HMGB1 induces cell cycle arrest and senescence in association with p21 (Waf1/Cip1) up-regulation via a p53-independent, Sp1-dependent pathway. *Oncotarget*. 2014 Aug 15;5(15):6387-403. doi: 10.18632/oncotarget.2201. PMID: 25051367; PMCID: PMC4171638.
107. Wang H, Bloom O, Zhang M, Vishnubhakat JM, Ombrellino M, Che J, Frazier A, Yang H, Ivanova S, Borovikova L, Manogue KR, Faist E, Abraham E, Andersson J, Andersson U, Molina PE, Abumrad NN, Sama A, Tracey KJ. HMG-1 as a late mediator of endotoxin lethality in mice. *Science*. 1999 Jul 9;285(5425):248-51. doi: 10.1126/science.285.5425.248. PMID: 10398600.
108. Chen R, Kang R, Tang D. The mechanism of HMGB1 secretion and release. *Exp Mol Med*. 2022 Feb;54(2):91-102. doi: 10.1038/s12276-022-00736-w. Epub 2022 Feb 25. PMID: 35217834; PMCID: PMC8894452.
109. Min HJ, Kim JH, Yoo JE, Oh JH, Kim KS, Yoon JH, Kim CH. ROS-dependent HMGB1 secretion upregulates IL-8 in upper airway epithelial cells under hypoxic condition. *Mucosal Immunol*. 2017 May;10(3):685-694. doi: 10.1038/mi.2016.82. Epub 2016 Sep 14. PMID: 27624778.

110. Davalos AR, Kawahara M, Malhotra GK, Schaum N, Huang J, Ved U, Beausejour CM, Coppe JP, Rodier F, Campisi J. p53-dependent release of Alarmin HMGB1 is a central mediator of senescent phenotypes. *J Cell Biol.* 2013 May 13;201(4):613-29. doi: 10.1083/jcb.201206006. Epub 2013 May 6. PMID: 23649808; PMCID: PMC3653366
111. Aird KM, Iwasaki O, Kossenkov AV, Tanizawa H, Fatkhutdinov N, Bitler BG, Le L, Alicea G, Yang TL, Johnson FB, Noma KI, Zhang R. HMGB2 orchestrates the chromatin landscape of senescence-associated secretory phenotype gene loci. *J Cell Biol.* 2016 Nov 7;215(3):325-334. doi: 10.1083/jcb.201608026. Epub 2016 Oct 31. PMID: 27799366; PMCID: PMC5100296.
112. Zirkel A, Nikolic M, Sofiadis K, Mallm JP, Brackley CA, Gothe H, Drechsel O, Becker C, Altmüller J, Josipovic N, Georgomanolis T, Brant L, Franzen J, Koker M, Gusmao EG, Costa IG, Ullrich RT, Wagner W, Roukos V, Nürnberg P, Marenduzzo D, Rippe K, Papantonis A. HMGB2 Loss upon Senescence Entry Disrupts Genomic Organization and Induces CTCF Clustering across Cell Types. *Mol Cell.* 2018 May 17;70(4):730-744.e6. doi: 10.1016/j.molcel.2018.03.030. Epub 2018 Apr 26. PMID: 29706538.
113. Jung HJ, Coffinier C, Choe Y, Beigneux AP, Davies BS, Yang SH, Barnes RH 2nd, Hong J, Sun T, Pleasure SJ, Young SG, Fong LG. Regulation of prelamin A but not lamin C by miR-9, a brain-specific microRNA. *Proc Natl Acad Sci U S A.* 2012 Feb 14;109(7):E423-31. doi: 10.1073/pnas.1111780109. Epub 2012 Jan 30. PMID: 22308344; PMCID: PMC3289373.
114. Shimi T, Pflieger K, Kojima S, Pack CG, Solovei I, Goldman AE, Adam SA, Shumaker DK, Kinjo M, Cremer T, Goldman RD. The A- and B-type nuclear lamin networks: microdomains involved in chromatin organization and transcription. *Genes Dev.* 2008 Dec 15;22(24):3409-21. doi: 10.1101/gad.1735208. PMID: 19141474; PMCID: PMC2607069.
115. Spann TP, Goldman AE, Wang C, Huang S, Goldman RD. Alteration of nuclear lamin organization inhibits RNA polymerase II-dependent transcription. *J Cell Biol.* 2002 Feb 18;156(4):603-8. doi: 10.1083/jcb.200112047. Epub 2002 Feb 18. PMID: 11854306; PMCID: PMC2174089
116. Moir RD, Spann TP, Herrmann H, Goldman RD. Disruption of nuclear lamin organization blocks the elongation phase of DNA replication. *J Cell Biol.* 2000 Jun 12;149(6):1179-92. doi: 10.1083/jcb.149.6.1179. PMID: 10851016; PMCID: PMC2175110.
117. Tang CW, Maya-Mendoza A, Martin C, Zeng K, Chen S, Feret D, Wilson SA, Jackson DA. The integrity of a lamin-B1-dependent nucleoskeleton is a fundamental determinant of RNA synthesis in human cells. *J Cell Sci.* 2008 Apr 1;121(Pt 7):1014-24. doi: 10.1242/jcs.020982. Epub 2008 Mar 11. PMID: 18334554.
118. Zheng X, Kim Y, Zheng Y. Identification of lamin B-regulated chromatin regions based on chromatin landscapes. *Mol Biol Cell.* 2015 Jul 15;26(14):2685-97. doi: 10.1091/mbc.E15-04-0210. Epub 2015 May 20. PMID: 25995381; PMCID: PMC4501365.
119. Shimi T, Butin-Israeli V, Adam SA, Hamanaka RB, Goldman AE, Lucas CA, Shumaker DK, Kosak ST, Chandel NS, Goldman RD. The role of nuclear lamin B1 in cell proliferation and senescence. *Genes Dev.* 2011 Dec 15;25(24):2579-93. doi: 10.1101/gad.179515.111. Epub 2011 Dec 8. PMID: 22155925; PMCID: PMC3248680.
120. Dreesen O, Chojnowski A, Ong PF, Zhao TY, Common JE, Lunny D, Lane EB, Lee SJ, Vardy LA, Stewart CL, Colman A. Lamin B1 fluctuations have differential effects on cellular proliferation and senescence. *J Cell Biol.* 2013 Mar 4;200(5):605-17. doi: 10.1083/jcb.201206121. Epub 2013 Feb 25. PMID: 23439683; PMCID: PMC3587829.
121. Barascu A, Le Chalony C, Pennarun G, Genet D, Imam N, Lopez B, Bertrand P. Oxidative stress induces an ATM-independent senescence pathway through p38 MAPK-mediated lamin B1 accumulation. *EMBO J.* 2012 Mar 7;31(5):1080-94. doi: 10.1038/emboj.2011.492. Epub 2012 Jan 13. PMID: 22246186; PMCID: PMC3297999.

122. Atadja P, Wong H, Veillete C, Riabowol K. Overexpression of cyclin D1 blocks proliferation of normal diploid fibroblasts. *Exp Cell Res* 1995; 217: 205–216.
123. Garkavtsev I, Hull C, Riabowol. Molecular aspects of the relationship between cancer and aging: tumor suppressor activity during cellular senescence. *Exp Gerontology* 1998; 33: 81–94.
124. Dulic V, Drullinger LF, Lee E, Reed SI, Stein GH. Altered regulation of G1 cyclins in senescent human fibroblasts: accumulation of inactive cyclin E-cdk2 and cyclin D1-cdk4 complexes. *Proc Natl Acad Sci USA* 1993; 90: 11034–11038.

Acknowledgments

First and foremost, I would like to thank my first examiner for giving me the opportunity to do my Doctoral thesis at the Institute of Toxicology in Mainz. I am grateful for the trust placed in me and for all the help I received during my time working in his working group.

I would like to thank my second corrector.

I would like to extend gratitude to the technical staff of the Institute of Toxicology for their continuous helpfulness, providing their considerable expertise in matters of lab operations and handling of all the problems that come up in the day to day of experimentation.

I would also like to thank the other undergrads and doctoral students who took time out of their busy days to teach me important tasks, as well as answered my many questions.

Finally, I thank my family and friends for accompanying me through all of it.

LEBENS LAUF

Studium

2015-2022

Studium der Humanmedizin an der Johannes Gutenberg-Universität Mainz

2022

2. Staatsexamen (M3: Note 3)

2021-2022

Praktisches Jahr an der Uniklinik Mainz;
Schwerpunkte:

- Pathologie
- Chirurgie mit Einsatz in der Orthopädie, Allgemein-Viszeral und Thoraxchirurgie sowie Herz-Thorax-Gefäßchirurgie
- Innere mit Einsatz in der Hämatookologie und auf der Leberstation

2021

1. Staatsexamen (M2: Note 3)

2018

Physikum (M1: Note 2)

Berufsausbildung

2012-2015

Ausbildung zum Pharmazeutisch-technischen Assistenten an der Schule für Gesundheit und Soziales Jena

2015

Bundesfreiwilligendienst am Uniklinikum Jena

Schulbildung

1999 –2003

Georgen – Grundschule Eisenach

2003 – 2012

Ernst Abbe Gymnasium Eisenach
Abschluss 2012: Abitur

2009/2010

High School Year in Nova Scotia

